A Distinctive Cytoplasmic Tail Contributes to Low Surface Expression and Intracellular Retention of the Patr-AL MHC class I molecule[1]

Running title: INTRACELLULAR RETENTION OF PATR-AL

Ana Goyos*[†‡], Lisbeth A. Guethlein*, Amir Horowitz*[†‡], Hugo G. Hilton*, Michael Gleimer*[†‡2], Frances M. Brodsky[§3] and Peter Parham*[†‡4]

* Department of Structural Biology, Stanford University School of Medicine, Stanford, CA, 94305, USA

[†] Department of Microbiology & Immunology, Stanford University School of Medicine, Stanford, CA, 94305, USA

[‡] Stanford Immunology, Stanford University School of Medicine, Stanford, CA, 94305, USA

[¶] Departments of Bioengineering & Therapeutic Sciences, Pharmaceutical Chemistry and Microbiology & Immunology, University of California San Francisco

ABSTRACT

(247 words)

Chimpanzees have orthologs of the six, fixed, functional human *MHC class I* genes. But in addition, the chimpanzee has a seventh functional gene, *Patr-AL*, which is not polymorphic but contributes substantially to population diversity by its presence on only 50% of *MHC* haplotypes. The ancestral *AL* gene emerged long before the separation of human and chimpanzee ancestors and then subsequently and specifically lost function during human evolution, but was maintained in chimpanzees. Patr-AL is an alloantigen that participates in negative and positive selection of the T-cell repertoire. The three-dimensional structure and the peptide-binding repertoire of Patr-AL and HLA-A*02 are surprisingly similar. In contrast, the expression of these two molecules is very different as shown using specific monoclonal and polyclonal antibodies made against Patr-AL. Peripheral blood cells and B cell lines express low levels of Patr-AL at the cell surface. Higher levels are seen for 221-cell transfectants expressing Patr-AL, but in these cells a large majority of Patr-AL molecules are retained in the early compartments of the secretory pathway: mainly the endoplasmic reticulum but also cis-Golgi. Replacing the cytoplasmic tail of Patr-AL with that of HLA-A*02 increased the cell-surface expression of Patr-AL substantially. Four substitutions distinguish the Patr-AL and HLA-A*02 cytoplasmic tails. Systematic mutagenesis showed that each substitution contributes changes in cell-surface expression. The combination of residues present in Patr-AL appears unique, but each individual residue is present in other primate MHC class I molecules, notably MHC-E, the most ancient of the functional human MHC class I molecules.

INTRODUCTION

The selective pressures imposed by diverse, fast-evolving pathogens cause the MHC class I genes of their mammalian hosts also to evolve rapidly (1). As a consequence there is considerable species-specific character to *MHC class I* gene families. Characteristics shared by most mammalian species are highly polymorphic 'classical' MHC class I molecules that engage highly variable types of lymphocyte receptor and conserved 'non-classical' MHC class I molecules that engage conserved types of lymphocyte receptors. Of the six human *MHC class I* genes that are functional, *HLA-A, -B* and *–C* are highly polymorphic and provide ligands for the αβ T-cell receptors of CD8 T cells and for the killer cell immunoglobulin-like receptors (KIR) of NK cells. In contrast, the *HLA-E, -F* and *–G* genes exhibit little variation. HLA-E is the ligand for the CD94:NKG2A and CD94:NKG2C receptors of NK cells (2), which complement and collaborate with the KIR. By comparison the function of HLA-F is poorly understood, but it could serve as a chaperone that transports unfolded HLA class I molecules back from the cell surface to the cell's interior (3). HLA-G is the most specialized, being expressed only by extravillous trophoblast during pregnancy (4) and monocytes (5). Cooperative interactions between HLA-G and the KIR2DL4 and LILRB1 receptors of uterine NK cells are necessary for the development of the placenta and the success of reproduction (6).

Counterparts to the HLA class I genes are restricted to simian primates, and the chimpanzee (*Pan troglodytes*) is has orthologs of all six expressed *HLA class I* genes (7). For some 50% of chimpanzee *MHC* haplotypes, these genes (*Patr-A, -B, -C, -E, -F* and *–G*) are the only expressed MHC class I genes, but the other 50% of haplotypes have a seventh expressed gene, *Patr-AL*, that is within an additional ~125kb block of genomic DNA that is next to the 80kb block

containing the *Patr-A* gene (8). More closely related to *Patr-A* than the other expressed genes, *Patr-AL* is one of a group of *A*-related genes (hence the name *A-like*) that includes the non-functional *MHC-H* and *MHC-J* genes (9). Although not yet proven, there is evidence for the existence of two forms of human *MHC* haplotype that correspond to the *Patr-AL*$^{+}$ and *Patr-AL*$^{-}$ chimpanzee haplotypes (8). Called *HLA*-Y, the human equivalent of *Patr-AL* is non-functional and contains a 5' region of high sequence similarity with *Patr-AL* that is recombined with a 3' region from another *A*-related gene (8). Neither *Patr-AL* nor *HLA-Y* exhibit significant polymorphism. Patr-AL originated long before the separation of human and chimpanzee ancestors (8, 9), and was specifically inactivated during human evolution. Such inactivation could have been driven by selection or by the demographic factors of population bottleneck and genetic drift. Study of Patr-AL will therefore define an immune system component that humans have lost.

Patr-AL forms a heterotrimeric complex with β_2-m and nonamer peptides to give a three-dimensional structure in which the Cα traces of the H chain and β2-m superimpose with their counterparts in other HLA class I structures (8). The peptide-binding specificity of Patr-AL is essentially the same as that of HLA-A*02, although the two molecules differ by >40 amino-acid substitutions of which 30 are in the α_1 and α_2 domains and 13 are predicted to contact peptide (8). These properties suggest that Patr-AL, like HLA-A and Patr-A, presents peptide antigens to αβ T cell receptors. Supporting this hypothesis, Patr-AL is an alloantigen recognized by the highly specific cytotoxic CD8 αβT cells that are present in chimpanzees lacking Patr-AL (8). This implies that Patr-AL is expressed in the thymus and mediates negative selection.

The major structural difference between Patr-AL and other human and chimpanzee MHC class I molecules is the upper face of the α helix of the α_2 domain, which is unusually electropositive and makes Patr-AL exceptional in having a basic isoelectric point (8). Previous preliminary analysis of mRNA levels indicated that the expression of Patr-AL was either very low or restricted to a minority of peripheral blood mononuclear cells (PBMC) (9). In the investigation reported here we made antibodies against Patr-AL and used them to study both endogenous Patr-AL protein expression as well as recombinant Patr-AL stably expressed in an MHC class I-deficient cell line and compared its expression with the well characterized human HLA-A*02 protein.

MATERIALS AND METHODS

Plasmids and Mutagenesis

Expression vectors were constructed by using PCR to amplify exons 1-8 of Patr-AL*01:01:01 and HLA-A*02:07 from plasmids (8, 9) and cloning the amplicons into the *HindIII* and *XbaI* sites of the mammalian expression vector pcDNA3.1+ (Invitrogen Life Technologies, Grand Island, NY), which drives expression via the CMV promoter. Patr-AL contains a methionine at the second position of the leader sequence peptide. A mutated construct was generated to express a threonine at that position (P2T). This mutation causes unstable binding of the leader peptide to HLA-E, resulting in poor cell surface expression of HLA-E, preventing binding to CD94:NKG2A/C.

Vectors containing FLAG-tagged Patr-AL and HLA-A*02 were generated by inserting a modified 3xFLAG tag (DYKDHDGDYKDHDIDYKDDDDK) between the signal sequence (encoded by exon 1) and the alpha 1 domain (encoded by exon 2) by a three-step PCR approach. All amplifications were with 0.2µM of each primer, 0.2mM total dNTPs, 1x enzyme buffer, 1.5mM $MgCl_2$, 2.5 units of HotStarTaq *Plus* DNA polymerase (Qiagen, Venlo, Netherlands). An exon 1 and first half of the 3xFLAG tag fragment (with 5' *HindIII* site) was amplified from a cDNA clone by using primers *HindIII*-AL-L-KZ-F or *HindIII*-A0207-L-KZ-F and 3xFLAG-ALL-R (primers listed in Figure S1) with amplification conditions of 5min at 95°C, 35 cycles of 30sec at 94°C, 30sec at 62°C, and 40sec at 72°C followed by a final 10min extension at 72°C. A second fragment consisting of the second half of the 3xFLAG and exons 2-8 (with 3' *XbaI* site) was amplified from a cDNA clone by using primers 3xFLAG-AL-F or 3xFLAG-A-F and XbaI_AL-A_Cyt_R with amplification conditions of 5min at 95°C, 35 cycles of 30sec at 94°C,

30sec at 62°C, and 1min10sec at 72°C followed by a final 10min extension at 72°C. The 3xFLAG primers were designed with a 22bp overlap allowing them to join during the third PCR step. The two amplified fragments were purified by gel extraction (Qiagen). These two fragments were joined and amplified from 1µl each of gel-purified PCR product by using primers *HindIII*-AL-L-KZ-F or *HindIII*-A0207-L-KZ-F and *XbaI*_AL-A_Cyt_R with amplification conditions of 5min at 95°C, 35 cycles of 30sec at 94°C, 1min25sec at 62°C, and 40sec at 72°C followed by a final 10min extension at 72°C. Purified PCR products consisting of exon1-3xFLAG-exons2-8 were digested with *HindIII* and *XbaI*, cloned into pcDNA3.1+ and the sequence determined (MCLAB, South San Francisco, CA).

In order to mutate specific residues in the transmembrane and cytoplasmic tails of 3xFLAG-tagged-Patr-AL or -HLA-A*02, site-directed mutagenesis (QuikChange Lightning Multi Site-Directed Mutagenesis Kit, Agilent Technologies, Santa Clara, CA) was performed following the manufacturer's protocol. Mutagenesis primers (Figure S2) were designed using Agilent Technologies' QuikChange Primer Design website (http://www.genomics.agilent.com/primerDesignProgram.jsp) and synthesized by the Protein and Nucleic Acid Core Facility (Stanford University). All constructs were sequenced (MCLAB), using T7 forward and BGH reverse primers, to assess the accuracy of the insert.

Preparation of a monoclonal antibody specific for native Patr-AL

Patr-AL-specific antibodies were generated by immunizing 10 BALB/c mice with soluble complexes of recombinant Patr-AL extracellular domains, β2m and the ALDKATVLL peptide. Mice were primed at day 0 intraperitoneally with 100µg of recombinant Patr-AL complexes in

complete Freund's adjuvant (Sigma-Aldrich, St. Louis, MO) and boosted similarly with antigen in Incomplete Freund's adjuvant (Sigma-Aldrich) on days 14, 28, and 56. Serum antibody titers were measured by ELISA using immobilized recombinant Patr-AL as antigen. The spleen from the mouse having the highest titer of antibodies was harvested on day 62, and fusion of splenocytes with FOX-NY myeloma cells (ATCC, Manassas, VA) was performed for 5min at a 5:1 ratio in PEG-3350 (Roche, Nutley, NJ). Hybridoma cells were cloned by limiting dilution or by single-cell sorting into 96-well plates on a FACSVantage DiVa instrument (Becton-Dickinson, Santa Clara, CA) at the Stanford Core FACS facility. Clones were grown in the presence of BALB/c feeder splenocytes in Advanced DMEM (Invitrogen, Carlsbad, CA) supplemented with 20% FetalClone I HyClone (GE Healthcare, Logan, UT), pyruvate (Invitrogen), and L-Glutamine (Invitrogen). Hybridoma clones were selected using the hypoxanthine/aminopterin/thymidine (HAT) supplement (Invitrogen). Seven days after fusion, hybridoma supernatants were screened by ELISA using soluble recombinant Patr-AL-covered plates. The 96 hybridomas giving strongest binding to Patr-AL were chosen for expansion and screening by flow cytometry. In screening, the hybridoma supernatants were tested for binding to HLA class I-deficient 221 cells and to a panel of 221 cell transfectants, each expressing a single human or chimpanzee MHC-A allotype. These comprised human HLA-A*01:01, A*02:01, A*02:07, and A*03:01, and chimpanzee Patr-A*0:402, A*05:01, A*06:01, A*10:01, A*11:01, A*13:01, A*16:01, and A*20:01. Monoclonal antibody (mAb) 10A5 was found to be the most specific and most sensitive, and was of the IgG1 heavy chain isotype and the κ light chain isotype. All experiments were approved by Stanford's Administrative Panel on Laboratory Animal Care (APLAC).

The specificity of the 10A5 mAb was further assessed using the LabScreen Group 1 Luminex assay (One Lambda, Canoga Park, CA) as described previously (10). In this assay 97 beads, each coated with a different HLA-A, –B or –C allotype, were tested for binding to 10A5. This panel of HLA allotypes represents a broad range of HLA-A, –B and –C variants. Although all the bead-coated HLA allotypes bound to W6/32, an antibody that reacts with all HLA class I molecules, none of the 97 HLA-A and –B allotypes bound to 10A5.

Preparation of a polyclonal antibody specific for unfolded Patr-AL

A Patr-AL-specific rabbit polyclonal antiserum (ALpoly) was raised (Anaspec, Inc, Fremont, CA) against the synthetic peptide QETQISKVYAQNDRVN, corresponding to residues 86-101 of Patr-AL. This sequence has the highest divergence from both Patr-A and HLA-A sequences. A cysteine was added to the C-terminus of the peptide, which enabled peptide-conjugates to be made with keyhole limpet hemocyanin and bovine serum albumin using hydroxysuccinimide. Antisera were raised in two rabbits according to approved company protocols. The antisera were assayed by ELISA using immobilized peptide as the antigen. The rabbit with higher serum titer was bled and Patr-AL-specific antibodies affinity-purified from the serum using immobilized peptide. On Western blots the resulting polyclonal antibody was shown to be highly specific for Patr-AL, failing to recognize Patr-A.

Cells, cell lines and transfections

Epstein-Barr virus-transformed chimpanzee B cell lines from both Patr-AL^+ and Patr-AL^- individuals were generated in our laboratory as described previously (9). Blood samples were obtained from common chimpanzees housed at Yerkes Regional Primate Center (Atlanta, GA).

PBMCs were isolated by ficoll density gradient separation (Ficoll-Paque PLUS, GE Healthcare) and cryopreserved in 90% heat-inactivated fetal bovine serum (HI-FBS, Gemini Bio-Products) + 10% DMSO (EMD Millipore, Billerica, MA). Cryopreserved PBMC were thawed and washed once in complete RPMI medium, re-suspended at a concentration of 2 x 10^6 cells per microliter and allowed to recover overnight (15 hours) at 37°C before performing any *in vitro* experiments.

Individual Patr-AL, HLA-A*02 and mutant cDNAs in the pcDNA3.1+ vector were stably transfected into the MHC-A, -B, and -C-deficient cell-line 721.221 (subsequently referred to as 221 cells). 2 x 10^6 221 cells were transfected in 100µl of Cell Line Nucleofector® Kit V (Lonza Group) using program A-024 in a Nucleofector™ 2b Device (Lonza Group, Basel, Switzerland) with 2µg of linearized DNA. Transfected 221 cells were mixed with 500µl complete RPMI (RPMI-1640 (Gibco®/Life technologies, Grand Island, NY) + 10% HI-FBS, 2mM L-Glutamine and antibiotics (penicillin [100units/ml] and streptomycin [100µg/ml]), Gibco®/Life technologies)) and 200µl were plated into 3 wells of a 96-well round-bottom plate. Four weeks later, successfully transfected 221 were expanded and sorted for positive MHC cell surface expression using the class I-specific Ab W6/32.

HeLa cells (ATCC Cell Lines) were plated in 24-well plates at 5 x 10^4 cells/well in 500µl of complete DMEM (DMEM (Gibco®/Life technologies) + 10% HI-FBS, 2mM L-Glutamine, 100 units/ml penicillin and 100µg/ml streptomycin) for 24hrs. Cells were then transfected with 1µg of a pcDNA3.1+ vector encoding FLAG-tagged Patr-AL, HLA-A or mutant allotypes and 3µl of the FuGENE® 6 transfection reagent (Promega, Madison, WI) in 25µl Opti-MEM (Gibco®/Life technologies) per well. 48h after transfection, adherent cells were dissociated from the wells

using 200µl 0.05% trypsin EDTA solution (Gibco®/Life technologies) for staining using a 3xFLAG-specific FITC-conjugated monoclonal antibody (M2-FITC, Sigma-Aldrich) and analysis by flow cytometry.

Immunoprecipitation and endoglycosidase H treatment

Patr-AL was immunoprecipitated from stable 221-Patr-AL transfectants with the mAb 10A5, using the Dynabeads® Co-Immunoprecipitation Kit (Invitrogen) and the manufacturer's protocol. Briefly, 10µg of 10A5 were coupled overnight to 1mg of Dynabeads® M-270 Epoxy. For each immunoprecipitation (IP) experiment, 1.5mg of antibody-coupled beads were used to IP Patr-AL from NP40 cell lysates of 150mg of cells. Following the recommended washes, samples were subjected to Endoglycosidase H (EndoH, New England Biolabs, Ipswich, MA) treatment. 1000U of EndoH in G5 buffer was used to digest 5µl of immunoprecipitate at 37°C for one hour. For protein blotting, samples were heated at 95°C for 5min, then separated by SDS-PAGE (BioRad, Hercules, CA) and analyzed by Western blot using ALpoly at a concentration of 0.5µg/ml.

Immunofluorescence and confocal microscopy

221-Patr-AL cells plated at 3.5 x 10^5 cells/well of a 24-well plate in 500µl complete RPMI on a 12 mm Round No. 1 German Glass Poly-D-Lysine coated glass coverslip (BD Biosciences, San Jose, CA) were allowed to attach for 1 hour at 37°C. Cells were then fixed with a mixture of 70% methanol and 30% acetone for 10min on ice followed by permeabilization for 1min with cold acetone. After washing wells three times with DPBS (containing calcium chloride and magnesium chloride, Gibco®), cells were blocked for 15min with cold Blocking Buffer (DPBS

containing 2% heat inactivated goat serum, 1% BSA, 0.1% cold fish skin gelatin, 0.02% SDS, 0.1% Nonidet P-40 and 0.05% sodium azide, pH 7.2). Cells were then stained with 5µg/mL of primary antibodies against Patr-AL (ALpoly), Invariant chain (PIN.1, Abcam, Cambridge, England), *cis*-Golgi (GM130, BD Biosciences) or HLA-DR (L243, BD Biosciences) diluted in Blocking Buffer and incubated overnight at 4°C with gentle agitation. After washing with Blocking Buffer, cells were incubated with 4µg/mL of goat anti-rabbit IgG Alexa Fluor 488, goat anti-mouse IgG1 Alexa Fluor 555 or goat anti-mouse IgG2a Alexa Fluor 647 (Molecular Probes, Eugene, OR) secondary antibodies in Blocking Buffer for 1hr at 4°C with gentle shaking. Cells were then washed in Blocking Buffer, followed by DPBS and coverslips were mounted for microscopy in ProLong Gold antifade reagent (Life Technologies). Secondary antibody specificity was assessed by controls in which primary antibody was omitted.

Cells processed for immunofluorescence were analyzed by confocal laser-scanning microscopy using an upright system (DM6000, SP5; Leica) with an oil immersion objective (63x, 1.3NA; HCX Plan Apochromat; Leica, Solms, Germany) and argon (488) and HeNe (543 and 633) lasers. Images were acquired using LAS AF SP5 software (Leica) in sequential scan mode with a 400-Hz scan rate, line averages of two, and a 512 × 512–pixel resolution. Z-stacks were collected at 0.3µm intervals. The same settings were maintained for all samples within an experiment. Raw images were processed using Volocity (PerkinElmer, Waltham, MA) by applying a fine filter to improve image quality. Quantitative colocalization analysis was performed on processed images by calculating the Pearson's correlation coefficient using the staining intensity of voxels falling within the region of interest (ROI) identified using the Lasso tool in Volocity. The automatically selected ROI from individual channels were then overlaid and analyzed. A value

of 0 represents no colocalization, whereas -1 represents negative colocalization and 1 represents positive colocalization.

Flow cytometry

Patr-AL and HLA-A*02 were detected on the surface of stably transfected 221 cells by staining with mAbs 10A5 and BB7.2 (BD Biosciences), respectively, at 5µg/ml in 50µl of FACS Buffer (1mM EDTA, 1% BSA and 0.04% azide in PBS). W6/32 (purified in our laboratory) was used at 5µg/ml as a pan-MHC class I antibody. After 3 washes with FACS Buffer, a goat anti-mouse IgG Alexa Fluor 488 (Molecular Probes) secondary antibody, at a concentration of 4ug/ml, was used to stain the cells. After 3 more washes with FACS Buffer, cells were resuspended in FACS Buffer containing 2mM propidium iodide (BD Biosciences) and fluorescence measurements were acquired using an Accuri C6 cytometer (BD Biosciences).

To detect intracellular Patr-AL, 221 transfectants were fixed with a mixture of 70% methanol and 30% acetone for 10min on ice, washed 3 times with Intracellular FACS Buffer (IFB: 1% BSA, 2% heat inactivated goat serum, 0.1% cold fish skin gelatin and 0.05% sodium azide, in PBS at pH 7.2), after which one aliquot of cells was permeabilized for 10min on ice using IFB supplemented with 0.02% SDS and 0.1% Nonidet P-40, and another aliquot was not permeabilized. From this point on, the permeabilized cells were washed with IFB containing Nonidet P-40 and SDS, whereas the unpermeabilized cells were washed with IFB only. Fixed and permeabilized cells were then stained with 100µl of 10A5 primary antibody at 5µg/ml in IFB, washed 3 times and subsequently stained with goat anti-mouse IgG Alexa Fluor 488 at 4µg/ml. After 3 more washes with IFB, cells were resuspended in IFB containing 2mM

propidium iodide (BD Biosciences) and fluorescence measurements using an Accuri C6 cytometer.

We examined the cell-surface expression of 36 3xFLAG-tagged Patr-AL, HLA-A*02 and individual transmembrane (TM) and cytoplasmic tail mutants in HeLa cells (ATCC Cell Lines). Transiently transfected HeLa cells were detached from the wells using 200µl 0.05% trypsin EDTA solution (Invitrogen) and the reaction was quenched with 1ml of complete RPMI. Detached cells were washed with Blocking Buffer and stained with 50µl of FITC-conjugated anti-FLAG mouse monoclonal IgG1, M2-FITC (Sigma-Aldrich) at a final concentration of 3µg/mL in FB. Following antibody staining, cells were washed 3 times with FB, and finally resuspended in FB containing 2mM propidium iodide and 2% paraformaldehyde. Cells expressing the FLAG-tagged mutants were detected by flow cytometry using an Accuri C6 cytometer (BD Biosciences). Expression levels of each mutant allotype were determined from the average median fluorescence intensity (mfi), of M2-FITC antibody-reactive cells. A minimum of three experiments were performed for each MHC allotype.

RESULTS

Most Patr-AL molecules made by B lymphoblastoid cells do not reach the cell surface

Previously we showed that the Patr-AL protein can be detected in chimpanzee peripheral blood mononuclear cells (PBMC) and B lymphoblastoid cell lines (BLCL), but at a much lower level than classical MHC class I molecules (9). To facilitate further study of Patr-AL expression, we made monoclonal antibodies from the B cells of mice immunized with soluble, recombinant Patr-AL. This antigen comprised the extracellular domains of Patr-AL, β_2-microglobulin and the nonamer Patr-AL-binding peptide ALDKATVLL (8). Of many monoclonal antibodies obtained, the 10A5 antibody was selected for use in this study because it binds strongly to Patr-AL and exhibits no detectable interaction with other MHC class I (Figure 1). Thus, 10A5 binds to HLA-A, B and C deficient 221 cells transfected with Patr-AL but not to untransfected 221 cells or to 221 cells transfected with either HLA-A or Patr-A (Figure 1A).

The W6/32 antibody recognizes an epitope shared by all human and chimpanzee MHC class I molecules (11). It thus binds to the small amount of HLA-E expressed on the surface of 221 cells (12). Transfection of 221 cells with wild-type Patr-AL, Patr-AL expressing a modified Leader peptide to prevent increased cell surface HLA-E expression (P2T), Patr-A or HLA-A causes cell-surface expression of these MHC class I molecules (Figure 1B). Transfection of 221 cells with either version of Patr-AL induces an increase in W6/32 binding that is about a third of that seen for Patr-A or HLA-A (Figure 1B). Binding of these same cell lines with an antibody specific to HLA-E (Figure 1C) demonstrates that there is not a significant difference of cell surface HLA-E expression between the two Patr-AL expressing cell lines. This result shows that unlike HLA-A and Patr-A, the majority of Patr-AL molecules made by the transfected 221 cells do not reach the

cell surface. This could arise from intracellular retention, intracellular degradation or a combination of these factors.

The exquisite specificity of the 10A5 antibody for Patr-AL is demonstrated by analysis to measure the binding of 10A5 to 97 HLA-A, -B and -C variants and comparing the results with the binding achieved by W6/32. This analysis was performed by using a panel of Luminex beads, in which each bead is coated with a different HLA class I molecule (13). Whereas the binding of W6/32 to the 97 beads varied between a fluorescence intensity of 17,715 and 28,136, the binding of 10A5 varied between 9 and 77 (Figure 1D). Thus none of the 31 HLA-A, 50 HLA-B and 16 HLA-C allotypes are bound significantly by the anti-Patr-AL mouse monoclonal antibody 10A5.

Chimpanzee cells and cell lines differ in their expression of cell-surface Patr-AL

Because the Patr-AL gene is carried by ~50% of chimpanzee MHC haplotypes, individual chimpanzees can have 0, 1 or 2 copies of the *Patr-AL* gene. B cell lines made from the lymphocytes of four Patr-AL$^-$ chimpanzees and six Patr-AL$^+$ chimpanzees were analyzed by flow cytometry for their capacity to bind the 10A5 antibody (Figure 2A). Cell lines from the Patr-AL$^-$ chimpanzees did not bind 10A5, whereas a variable but reproducible binding was observed for the cell lines from Patr-AL$^+$ chimpanzees (Figure 2A). We measured the frequency of 10A5 positive cells because the fluorescence staining intensity of the bulk populations were similar. Only a minority of cells bound the 10A5 antibody, the number varying between 1% and 13% of cells. Both Miss Eve and Ericka have two copies of Patr-AL; Miss Eve being homozygous and Ericka being heterozygous (9). Since this information is not known for the

other chimpanzee BLCL used in this study, we cannot exclude the possibility of a *Patr-AL* gene-dosage effect in augmenting Patr-AL's expression in Miss Eve and Ericka B cell lines.

Analogous results were obtained when PBMC from eight Patr-AL$^-$ chimpanzees and sixteen Patr-AL$^+$ chimpanzees were similarly analyzed, but the fraction of cells from Patr-AL$^+$ chimpanzees that stain with 10A5 is less than 3% (Figure 2C). In fact, most of the bulk PBMC populations we analyzed contained less than 1% of cells staining positive for 10A5, a value that is well within the background of the gating strategy used for this analysis. To test the possibility that Patr-AL was enriched in a particular subset of PBMC, we performed immunophenotyping experiments where we identified T cells, B cells, NK cells, monocytes and granulocytes, but did not observe such enrichment (data not shown). Chimpanzee PBMC were also stimulated *in vitro* with the cytokine IFN-γ, a compound known to upregulate MHC class I expression, and with a potent polyclonal T cell stimulator, the superantigen staphylococcal enterotoxin A (SEA), to determine whether an upregulation of cell surface Patr-AL could be detected. *In vitro* stimulation of chimpanzee PBMC with IFN-γ or SEA at different concentrations for 48 hours did not result in an increase in cell surface Patr-AL (data not shown). Despite the reduced levels of cell surface Patr-AL on chimpanzee BLCL and PBMC, these cells do express a constitutive level of classical class I molecules on their cell surface (Figures 2B and D), as expected. These results clearly show that Patr-AL, unlike classical MHC class I, is not constitutively expressed at cell surfaces.

To determine whether endogenous Patr-AL could be detected intracellularly, we used immunofluorescence staining and high-resolution confocal microscopy to detect Patr-AL in chimpanzee BLCL derived from Miss Eve (Figure 2E) or Faye (Figure 2F). In these experiments

Patr-AL was detected using a specific rabbit anti-Patr-AL polyclonal antibody (ALpoly). This antibody, which was raised against a synthetic peptide corresponding to residues 86-101 of the Patr-AL α_1 and α_2 domains, recognizes both native and denatured Patr-AL (see Materials and Methods). As a marker of the endoplasmic reticulum (ER), we used an antibody specific for the cytoplasmic tail of the MHC class II invariant chain. This antibody marks the ER and early secretory pathway, because the cytoplasmic tail becomes degraded when the invariant chain traffics from the secretory pathway to an endosomal compartment (14). A signal specific for Patr-AL is detected intracellularly in BLCL from a Patr-AL^{pos} donor, while no signal is detected in the BLCL derived from the Patr-AL^{neg}. These results suggest that Patr-AL is intracellularly localized.

Patr-AL is synthesized and sequestered inside B lymphoblastoid cells

For Patr-AL and HLA-A*02, which have remarkably similar structures and peptide-binding specificities (8), we compared the distribution of molecules between the cell surface and intracellular compartments (Figure 3). Transfected 221 cells expressing Patr-AL or HLA-A*02, under the control of the same promoter, were tested for binding 10A5 (Figure 3A) and the HLA-A*02-specific antibody BB7.2 (Figure 3B). Consistent with these specificities, the Patr-AL transfectant bound 10A5 but not BB7.2, whereas the HLA-A*02 transfectant bound BB7.2 but not Patr-AL. Furthermore, the cell-surface-binding to Patr-AL by 10A5 (Figure 3A) was only 6% that of HLA-A*02 to BB7.2 (Figure 3B). To assess the relative amounts of intracellular Patr-AL and HLA-A*02, aliquots of transfected 221 cells were either fixed, or first fixed and then permeabilized, prior to staining with the 10A5 and BB7.2 antibodies. Permeabilization dramatically increased the specific binding of 10A5 to the Patr-AL transfected cells (Figure 3C),

but did not similarly affect the binding of BB7.2 to HLA-A*02 (Figure 3D). Thus while similar amounts of Patr-AL and HLA-A*02 are made by the transfectants, since both are generated by expression under the control of the strong CMV promoter, >90% of HLA-A*02 is delivered to the cell surface, whereas >90% of Patr-AL is sequestered within the cell.

Patr-AL is retained within cells at an early stage in the secretory pathway

To identify the intracellular sites where Patr-AL is sequestered, we used immunofluorescence staining and high-resolution confocal microscopy to compare the intracellular distribution of Patr-AL with those of well-characterized intracellular markers. A significant co-localization of Patr-AL with the invariant chain was observed (Figure 4A), showing a retention of Patr-AL in the ER and early secretory pathway. In contrast, there was little co-localization of Patr-AL with the mature MHC class II molecules detected by the L243 monoclonal antibody (Figure 4B), most of which are not associated with the invariant chain (Figure 4C). Also observed was co-localization of Patr-AL with the Golgi matrix protein GM130, a cis-Golgi marker (Figure 4D), but to lesser extent (~45%) than the co-localization of Patr-AL with invariant chain (Figure 4A), suggesting that most of the intracellular Patr-AL is localized to the ER. Consistent with the results of flow cytometry (Figure 1A), a small amount of Patr-AL was visualized on the cell surface in analysis of transient HeLa transfectants by microscopy (Figure S3). These results therefore show that whereas small amounts of Patr-AL are observed on cell surfaces, most of the cellular Patr-AL is retained within the cell, mostly in the ER and to a lesser degree in the cis-Golgi.

To confirm the results of the microscopy experiments, we examined the maturity of the oligosaccharide attached to asparagine 86 of Patr-AL and hence whether Patr-AL has undergone posttranslational modification upon trafficking through the Golgi apparatus. Immunoprecipitation of Patr-AL with the 10A5 antibody was performed on lysates prepared from 221 cells and 221 cells transfected with Patr-AL. The precipitates were treated with endoglycosidase H, which removes immature, but not mature, N-linked oligosaccharides, and then subjected to SDS-PAGE and Western blotting using rabbit ALpoly. Analysis of the immunoprecipitates (Figure 4E left), as well as whole cell lysates (Figure 4E right), show that Patr-AL was detected, as expected, only in the Patr-AL transfected cells. On treatment with endoglycosidase H most, but not all, of the Patr-AL heavy chains were reduced in molecular weight and were thus sensitive to the enzyme (Figure 4E left). This in turn shows that most, but not all, Patr-AL molecules carry an immature N-linked oligosaccharide. This result is consistent with intracellular Patr-AL molecules being sequestered principally in the ER, and secondarily in the *cis*-Golgi.

To determine if Patr-AL molecules travel to endolysosomal compartments, we examined lysosomes, late endosomes and compartments containing mature MHC class II for the presence of Patr-AL. Patr-AL transfected 221 cells were stained with rabbit ALpoly, monoclonal MHC class II specific L243 and a monoclonal antibody specific for Lamp-1, a marker of late endosomes and lysosomes (Figure 4F). The extent of the colocalization between the three markers was quantified. A good correlation was observed between the presence of Lamp-1 and HLA-DR, but no correlation between the presence of Patr-AL and either Lamp-1 or HLA-DR (Figure 4G). As is well established (15), we find that mature MHC class II molecules do travel to

endolysosomal compartments. In contrast, we find no evidence for the movement of Patr-AL molecules from the ER to endolysosomal compartments during steady state conditions. In conclusion, these experiments (Figure 4) demonstrate that Patr-AL is actively retained at an early stage of the secretory pathway, which is predominantly in the ER but also includes the cis-Golgi.

In some circumstances, proteins that are retained in the ER can be brought to the cell surface by lowering the temperature below 37°C (16, 17). To test this possibility for Patr-AL, we subjected 221 transfectants expressing Patr-AL or HLA-A*02 to overnight culture at temperatures ranging from 21°C to 37°C. The expression of Patr-AL and HLA-A*02 was then determined by flow cytometry using the 10A5 and BB7.2 antibodies, respectively. Over this temperature range there was no difference in the cell-surface expression of HLA-A*02. In contrast, for Patr-AL we observed a trend in which there was an increase by 31% of cell surface expression as the temperature was lowered from 37°C to 27°C which then reversed as the temperature was further lowered to 21°C (Figure 5).

The distinctive cytoplasmic tail of Patr-AL is a cause of intracellular retention

One mechanism used to retain transmembrane proteins inside cells involves sequence motifs in the cytoplasmic tail that are bound by tethering or adaptor proteins (18-20). In examining the sequence of the Patr-AL cytoplasmic tail we found a modified tyrosine-based sorting signal, YFQA at positions 320-323, which would potentially affect endocytosis or trans-Golgi network sorting, but no dileucine-based endocytic protein sorting motifs, none of which would be relevant to the localization of Patr-AL in the early secretory pathway. Comparing the cytoplasmic tail sequences of MHC class I molecules from different species identified four

451 residues (phenylalanine 321, asparagine 326, serine 329 and glutamate 333) that appear unique
452 to Patr-AL (Figure 6A and S4). Moreover, these are the only four residues that distinguish the
453 cytoplasmic tails of Patr-AL and HLA-A*02. Remarkably, this combination of residues found in
454 Patr-AL's cytoplasmic tail is unique to Patr-AL and not found in cytoplasmic tail sequences of
455 the known Patr-AL orthologs (8), HLA-Y, Gogo-OKO and Popy-A, nor in any other
456 characterized MHC class I molecule (Figure S4). We therefore hypothesized that one or more of
457 these four residues contribute to the intracellular retention and low cell-surface expression of
458 Patr-AL.
459
460 To test this hypothesis we made Patr-AL and HLA-A*02 mutants in which their cytoplasmic
461 tails were swapped, the prediction being that mutant Patr-AL with the HLA-A*02 tail would
462 have higher cell-surface expression, whereas mutant HLA-A*02 with the Patr-AL tail would
463 have lower cell-surface expression. Stable 221 transfectants expressing the two recombinant
464 mutants and the two parental molecules were tested for their capacity to bind Patr-AL-specific
465 10A5 and HLA-A*02-specific BB7.2. Expression of the Patr-AL mutant with the HLA-A*02 tail
466 was 5.0 fold higher than that of Patr-AL (Figure 6B). Similarly, the cell-surface expression of
467 HLA-A*02 was 4.5 fold that of the HLA-A*02 mutant with the Patr-AL tail (Figure 6C). These
468 results were recapitulated by high resolution confocal microscopy analysis of transient HeLa
469 transfectants (Fig. S3). These results demonstrate that one or more of the four substitutions that
470 distinguish the cytoplasmic tails of Patr-AL and HLA-A*02 contribute to the differential cell-
471 surface expression of these two MHC class I molecules. However, these differences can only
472 account for approximately one third of the 13.4 fold difference in the expression of HLA-A*02

and Patr-AL in 221 transfectants (Figure 1C). Thus substitutions in other domains of the Patr-AL and HLA-A*02 proteins are also implicated in altering cell-surface expression.

The four residues that distinguish the cytoplasmic tail of Patr-AL all act to reduce cell-surface expression

To determine the effects of the four substitutions that distinguish the cytoplasmic tails of Patr-AL and HLA-A*02, we made sets of 16 Patr-AL and 16 HLA-A*02 mutants that represent all possible combinations of the dimorphisms at positions 321, 326, 329 and 333. To facilitate comparison of the cell-surface expression of these mutants, we included 3xFLAG epitopes at the amino-terminus of each mutant and parental allotype. These constructs were transiently transfected into HeLa cells and their cell surface expression assessed by flow cytometry using the M2 monoclonal antibody that recognizes the 3xFLAG epitope (Figure 7).

The cytoplasmic tail of Patr-AL is distinguished by phenylalanine 321 (F321), asparagine 326 (N326), serine 329 (S329) and glutamate 333 (E333). We compared the expression levels of Patr-AL cytoplasmic tail mutants upon step-wise mutagenesis from an HLA-A*02 (top of each panel) to a Patr-AL cytoplasmic tail (bottom of each panel). The results from the subset of Patr-AL mutants shown in Figure 7A allows us to assess how each individual residue influences the cell-surface expression of Patr-AL. Phenylalanine 321 has the strongest impact, accounting for around 50% of the effect in reduced surface expression of the Patr-AL tail. The other 50% is due to lesser contributions from the residues at positions 326, 329 and 333. Among the six combinations of two residue mutants, phenylalanine 321 and glutamate 333 give the greatest effect (Figure 7B), whereas among the four possible mutants combining three of the residues, it

is the combination of phenylalanine 321, serine 329 and glutamate 333 that is most effective (Figure 7C). However none of these mutants is as effective as the combination of all four residues present in the cytoplasmic tail of Patr-AL. Thus, for Patr-AL, while phenylalanine at position 321 plays a dominant role in the decrease of Patr-AL surface expression, each of the four Patr-AL cytoplasmic tail-specific residues have all made contributions in reducing the cell-surface expression of Patr-AL.

In similar analysis of the four substitutions that distinguish the HLA-A*02 cytoplasmic tail from that of Patr-AL, the presence of either serine 321, alanine 329 or aspartate 333 is sufficient to restore cell-surface expression to a level that is greater or equal to that of HLA-A*02. And the presence of serine 326 achieves 92% of wild-type HLA-A*02 expression (Figure 7C). Although individually the four residues have positive effects, in combinations they have more varied effects. Thus the combination of serine 321, serine 326 and aspartate 333 causes little increase of HLA-A*02 cell-surface expression over that seen with the full Patr-AL cytoplasmic tail mutant of HLA-A*02 (Figure 7A), and the combinations of either serine 326 or alanine 329 with aspartate 333 also have small effects (Figure 7B). In contrast there are several combinations of residues that raise the level of cell-surface expression well above that of HLA-A*02 (Figure 7A). Thus there are antagonistic and synergistic effects between the residues at positions 321, 326, 329 and 333 in HLA-A*02. These results suggest that for both Patr-AL and HLA-A, while polymorphisms in cytoplasmic tail residues contribute to differences in cell surface expression, there are other factors simultaneously regulating their surface expression.

Natural sequence variation in the transmembrane domain influences cell-surface expression

Because multiple factors are implicated in reducing cell-surface expression of Patr-AL, we investigated the effect of the single amino-acid difference that distinguishes the transmembrane (TM) domains of Patr-AL and HLA-A. At position 295 Patr-AL has valine and HLA-A*02 has glycine. Mutants were made, in which these residues were swapped, and analyzed using the same methods applied to the cytoplasmic tail mutants (Figure 8).

The substitution of valine for glycine at position 295 in Patr-AL has no significant effect on cell-surface expression. Neither did polymorphism at position 295 affect cell-surface expression of the Patr-AL mutant that has the cytoplasmic tail of HLA-A*02 (Figure 8). In contrast, mutating residue 295 from glycine to valine in HLA-A*02 increases the surface expression by 30%. This effect is not seen in the HLA-A*02 mutant that has both the transmembrane domain and the cytoplasmic tail of Patr-AL, and which gives identical cell-surface expression to HLA-A*02. However, the HLA-A*02 mutant with just the Patr-AL cytoplasmic tail has expression reduced by 32% (Figure 8). These results demonstrate that in contrast to Patr-AL, in HLA-A, both the transmembrane and cytoplasmic tail residues play a role in surface expression. This suggests that the cell surface expression of Patr-AL and HLA-A*02 are regulated by two different mechanisms and further establishes how natural substitutions in the transmembrane domain and cytoplasmic tail can antagonize or synergize in determining the level of cell-surface expression of MHC class I molecules.

DISCUSSION

To study the expression of Patr-AL we made a specific monoclonal antibody that binds to Patr-AL with high specificity but does not react with other human or chimpanzee MHC class I molecules. This antibody binds at a low level to small numbers of PBMC. Greater surface expression of Patr-AL occurs when human, class I-deficient 221 cells are transfected with *Patr-AL* expressed under control of the CMV promoter. For this reason, we used 221 transfectants to examine the cell surface expression and intracellular distribution of Patr-AL. A minority of Patr-AL molecules are detected at the cell surface (~10%), the majority being retained inside the cell within the endoplasmic reticulum (ER) and the cis-Golgi. This behavior contrasts with HLA-A*02, which is predominantly expressed at the cell surface. That a substantial majority of Patr-AL molecules are located within cells could explain, at least in part, the small amounts of Patr-AL detected on the surface of PBMC. In addition, the Patr-AL promoter could limit the extent of transcription in the cells in which Patr-AL is transcribed, but this has yet to be investigated.

The retention of Patr-AL in early compartments of the secretory pathway is likely to be an active process and one that could be critical to its immunological function. Precedents for the intracellular retention of MHC class I molecules are provided by human MR1 and mouse Qa-1 (21-23). MR1 binds to the vitamin B metabolites released by bacteria and yeast infecting mucosal tissue (24). On binding such antigens MR1 moves to the cell surface where it is recognized by mucosal-associated T cells. Qa-1 monitors antigen processing in the ER by being sensitive to a self-peptide called FL9 that only accumulates when the ER-resident aminopeptidase malfunctions (23). On binding to FL9, Qa-1 is released from the ER and translocates to the cell surface where it is recognized by cytotoxic T cells that kill the defective

cell (23). Both the examples of MR1 and Qa-1 retention rely on the unavailability of their ligands. While peptides that can be presented by Patr-AL are similar to those presented by HLA-A*02 (7) and are therefore readily available, it is still possible that Patr-AL may preferentially bind some type of modified peptide. To this end, it is noteworthy to mention the unusually electropositive patch on the alpha 2 domain of Patr-AL (7). We speculate that Patr-AL binds an electronegative macromolecule that is normally not available in the ER.

Underlying the intracellular retention of Patr-AL are four amino-acid substitutions that distinguish the cytoplasmic tails of Patr-AL and HLA-A*02. This was first appreciated by swapping the cytoplasmic tails of Patr-AL and HLA-A*02 and further dissected by mutagenesis at the four positions (321, 326, 329 and 333) that distinguish the two tails. In Patr-AL, each of the four residues acts to decrease cell-surface expression, suggesting a stepwise evolution that was driven by a continued process of selection for intracellular retention. The FNSE motif of Patr-AL is not shared with any other MHC class I molecule known. In hominoid MHC class I, N326 and E333 both occur, but not together. In Old World Monkey MHC class I molecules (Figure S4), all four residues occur but no more than two in any particular MHC class I variant. Residues F321, N326 and E333 occur in Old World Monkey MHC-B and S329 is present in MHC-E (Figure S4). In fact, all four residues of the Patr-AL motif are distributed among the MHC-E molecules of the simian primates (Figure S4). This observation, and knowledge that HLA-E is probably the oldest of the expressed MHC class I genes in simian primates (25, 26) raise the possibility that the FNSE motif first evolved at the MHC-E locus and was subsequently introduced into Patr-AL by recombination or gene conversion.

A variety of motifs that determine the intracellular movements and localization of MHC class I molecules have been identified (18) (Figure 9). For example, the cytoplasmic tail sequence of the classical MHC class I HLA-C contains a dihydrophobic internalization and lysosomal targeting signal (27) that contributes to its low cell surface expression, when compared to HLA-A and HLA-B. Cytoplasmic tails can also contain motifs essential for the protein's function and localization, such as the dihydrophobic motif in the cytoplasmic tail of MIC-A that determines its basolateral sorting (19, 28). The FNSE motif of Patr-AL involves different residues and is non-overlapping with other motifs (Figure 9). Thus the cytoplasmic tail of Patr-AL is seen to contain a unique sequence motif that is implicated in limiting cell surface expression. It is also notable that a single amino acid difference in the transmembrane domain has some contribution to the limitation of Patr-AL expression and that lowering the temperature of cells can partially induce Patr-AL expression. Thus, in addition to the strong retention motif defined, other features, such as interaction with accessory molecules and/or peptide binding could contribute to Patr-AL expression.

The cytoplasmic tails of HLA class I molecules are targets for viral proteins that subvert HLA class I function and thus prevent elimination of virus-infected cells by cytotoxic CD8 T cells (29). For example, the BILF1 protein of EBV prevents antigen-presenting HLA class I molecules from reaching the cell surface by directing them to lysosomes for degradation (30). Resistance to BILF1-mediated down-regulation is conferred by defined residues, cysteine 320, asparagine 327 and/or glutamate 334, in the cytoplasmic tail of HLA class I (31). Asparagine 326 and glutamate 333 in the FNSE motif of Patr-AL are predicted to prevent recognition by BILF1. Furthermore, phenylalanine 321 and asparagine 326 in Patr-AL's FNSE motif are predicted to prevent

608 recognition by the Nef proteins of human HIV and chimpanzee SIVcpz (32-35). These Nef
609 proteins bind to the cytoplasmic tail of MHC-A allotypes, including HLA-A*02, and deliver
610 them to lysosomes for degradation (36). Being resistant to the subversive actions of viral proteins
611 would allow Patr-AL to potentially function as an antigen-presenting molecule from where it
612 localizes in the early secretory pathway. For example, there are intracellular pathogens that
613 exploit this part of the secretory pathway for replication, such as *Legionella pneumophila* and
614 related species (37), which infect a wide variety of hosts, suggesting that Patr-AL may be well
615 placed to stimulate a cytotoxic T cell response against such organisms.

ACKNOWLEDGEMENTS

We thank the Yerkes Regional Primate Center for the samples of chimpanzee peripheral blood and the Stanford Microscopy Facility for use of their Leica SP5 upright confocal microscope. We also thank Bich Tien N. Rouse for expertise in generating the 10A5 monoclonal antibody specific for Patr-AL.

REFERENCES

1. Parham, P. 2005. MHC class I molecules and KIRs in human history, health and survival. *Nat Rev Immunol* 5: 201-214.
2. Lee, N., M. Llano, M. Carretero, A. Ishitani, F. Navarro, M. Lopez-Botet, and D. E. Geraghty. 1998. HLA-E is a major ligand for the natural killer inhibitory receptor CD94/NKG2A. *Proc Natl Acad Sci U S A* 95: 5199-5204.
3. Goodridge, J. P., A. Burian, N. Lee, and D. E. Geraghty. 2010. HLA-F complex without peptide binds to MHC class I protein in the open conformer form. *J Immunol* 184: 6199-6208.
4. Kovats, S., E. K. Main, C. Librach, M. Stubblebine, S. J. Fisher, and R. DeMars. 1990. A class I antigen, HLA-G, expressed in human trophoblasts. *Science* 248: 220-223.
5. Yang, Y., W. Chu, D. E. Geraghty, and J. S. Hunt. 1996. Expression of HLA-G in human mononuclear phagocytes and selective induction by IFN-gamma. *J Immunol* 156: 4224-4231.
6. Rouas-Freiss, N., R. M. Goncalves, C. Menier, J. Dausset, and E. D. Carosella. 1997. Direct evidence to support the role of HLA-G in protecting the fetus from maternal uterine natural killer cytolysis. *Proc Natl Acad Sci U S A* 94: 11520-11525.
7. Adams, E. J., and P. Parham. 2001. Species-specific evolution of MHC class I genes in the higher primates. *Immunological reviews* 183: 41-64.
8. Gleimer, M., A. R. Wahl, H. D. Hickman, L. Abi-Rached, P. J. Norman, L. A. Guethlein, J. A. Hammond, M. Draghi, E. J. Adams, S. Juo, R. Jalili, B. Gharizadeh, M. Ronaghi, K. C. Garcia, W. H. Hildebrand, and P. Parham. 2011. Although divergent in residues of the

643 peptide binding site, conserved chimpanzee Patr-AL and polymorphic human HLA-A*02
644 have overlapping peptide-binding repertoires. *J Immunol* 186: 1575-1588.
645 9. Adams, E. J., S. Cooper, and P. Parham. 2001. A novel, nonclassical MHC class I
646 molecule specific to the common chimpanzee. *J Immunol* 167: 3858-3869.
647 10. Hilton, H. G., and P. Parham. 2013. Direct binding to antigen-coated beads refines the
648 specificity and cross-reactivity of four monoclonal antibodies that recognize polymorphic
649 epitopes of HLA class I molecules. *Tissue antigens* 81: 212-220.
650 11. Brodsky, F. M., and P. Parham. 1982. Evolution of HLA antigenic determinants: species
651 cross-reactions of monoclonal antibodies. *Immunogenetics* 15: 151-166.
652 12. Lo Monaco, E., L. Sibilio, E. Melucci, E. Tremante, M. Suchanek, V. Horejsi, A.
653 Martayan, and P. Giacomini. 2008. HLA-E: strong association with beta2-microglobulin
654 and surface expression in the absence of HLA class I signal sequence-derived peptides. *J*
655 *Immunol* 181: 5442-5450.
656 13. Moesta, A. K., P. J. Norman, M. Yawata, N. Yawata, M. Gleimer, and P. Parham. 2008.
657 Synergistic polymorphism at two positions distal to the ligand-binding site makes
658 KIR2DL2 a stronger receptor for HLA-C than KIR2DL3. *J Immunol* 180: 3969-3979.
659 14. Ferrari, G., A. M. Knight, C. Watts, and J. Pieters. 1997. Distinct intracellular
660 compartments involved in invariant chain degradation and antigenic peptide loading of
661 major histocompatibility complex (MHC) class II molecules. *J Cell Biol* 139: 1433-1446.
662 15. Neefjes, J., M. L. Jongsma, P. Paul, and O. Bakke. 2011. Towards a systems
663 understanding of MHC class I and MHC class II antigen presentation. *Nat Rev Immunol*
664 11: 823-836.

16. Ljunggren, H. G., N. J. Stam, C. Ohlen, J. J. Neefjes, P. Hoglund, M. T. Heemels, J. Bastin, T. N. Schumacher, A. Townsend, K. Karre, and et al. 1990. Empty MHC class I molecules come out in the cold. *Nature* 346: 476-480.

17. Taner, S. B., M. J. Pando, A. Roberts, J. Schellekens, S. G. Marsh, K. J. Malmberg, P. Parham, and F. M. Brodsky. 2011. Interactions of NK cell receptor KIR3DL1*004 with chaperones and conformation-specific antibody reveal a functional folded state as well as predominant intracellular retention. *J Immunol* 186: 62-72.

18. Lizee, G., G. Basha, and W. A. Jefferies. 2005. Tails of wonder: endocytic-sorting motifs key for exogenous antigen presentation. *Trends Immunol* 26: 141-149.

19. Kozik, P., R. W. Francis, M. N. Seaman, and M. S. Robinson. 2010. A screen for endocytic motifs. *Traffic* 11: 843-855.

20. Hsu, K. C., S. Chida, D. E. Geraghty, and B. Dupont. 2002. The killer cell immunoglobulin-like receptor (KIR) genomic region: gene-order, haplotypes and allelic polymorphism. *Immunological reviews* 190: 40-52.

21. Miley, M. J., S. M. Truscott, Y. Y. Yu, S. Gilfillan, D. H. Fremont, T. H. Hansen, and L. Lybarger. 2003. Biochemical features of the MHC-related protein 1 consistent with an immunological function. *J Immunol* 170: 6090-6098.

22. Chua, W. J., S. Kim, N. Myers, S. Huang, L. Yu, D. H. Fremont, M. S. Diamond, and T. H. Hansen. 2011. Endogenous MHC-related protein 1 is transiently expressed on the plasma membrane in a conformation that activates mucosal-associated invariant T cells. *J Immunol* 186: 4744-4750.

686 23. Nagarajan, N. A., F. Gonzalez, and N. Shastri. 2012. Nonclassical MHC class Ib-
687 restricted cytotoxic T cells monitor antigen processing in the endoplasmic reticulum. *Nat*
688 *Immunol* 13: 579-586.
689 24. Kjer-Nielsen, L., O. Patel, A. J. Corbett, J. Le Nours, B. Meehan, L. Liu, M. Bhati, Z.
690 Chen, L. Kostenko, R. Reantragoon, N. A. Williamson, A. W. Purcell, N. L. Dudek, M. J.
691 McConville, R. A. O'Hair, G. N. Khairallah, D. I. Godfrey, D. P. Fairlie, J. Rossjohn, and
692 J. McCluskey. 2012. MR1 presents microbial vitamin B metabolites to MAIT cells.
693 *Nature* 491: 717-723.
694 25. Averdam, A., B. Petersen, C. Rosner, J. Neff, C. Roos, M. Eberle, F. Aujard, C. Munch,
695 W. Schempp, M. Carrington, T. Shiina, H. Inoko, F. Knaust, P. Coggill, H. Sehra, S.
696 Beck, L. Abi-Rached, R. Reinhardt, and L. Walter. 2009. A novel system of polymorphic
697 and diverse NK cell receptors in primates. *PLoS Genet* 5: e1000688.
698 26. Flugge, P., E. Zimmermann, A. L. Hughes, E. Gunther, and L. Walter. 2002.
699 Characterization and phylogenetic relationship of prosimian MHC class I genes. *J Mol*
700 *Evol* 55: 768-775.
701 27. Schaefer, M. R., M. Williams, D. A. Kulpa, P. K. Blakely, A. Q. Yaffee, and K. L.
702 Collins. 2008. A novel trafficking signal within the HLA-C cytoplasmic tail allows
703 regulated expression upon differentiation of macrophages. *J Immunol* 180: 7804-7817.
704 28. Suemizu, H., M. Radosavljevic, M. Kimura, S. Sadahiro, S. Yoshimura, S. Bahram, and
705 H. Inoko. 2002. A basolateral sorting motif in the MICA cytoplasmic tail. *Proc Natl Acad*
706 *Sci U S A* 99: 2971-2976.
707 29. Hansen, T. H., and M. Bouvier. 2009. MHC class I antigen presentation: learning from
708 viral evasion strategies. *Nat Rev Immunol* 9: 503-513.

30. Zuo, J., L. L. Quinn, J. Tamblyn, W. A. Thomas, R. Feederle, H. J. Delecluse, A. D. Hislop, and M. Rowe. 2011. The Epstein-Barr virus-encoded BILF1 protein modulates immune recognition of endogenously processed antigen by targeting major histocompatibility complex class I molecules trafficking on both the exocytic and endocytic pathways. *J Virol* 85: 1604-1614.

31. Griffin, B. D., A. M. Gram, A. Mulder, D. Van Leeuwen, F. H. Claas, F. Wang, M. E. Ressing, and E. Wiertz. 2013. EBV BILF1 evolved to downregulate cell surface display of a wide range of HLA class I molecules through their cytoplasmic tail. *J Immunol* 190: 1672-1684.

32. Cohen, G. B., R. T. Gandhi, D. M. Davis, O. Mandelboim, B. K. Chen, J. L. Strominger, and D. Baltimore. 1999. The selective downregulation of class I major histocompatibility complex proteins by HIV-1 protects HIV-infected cells from NK cells. *Immunity* 10: 661-671.

33. Kasper, M. R., J. F. Roeth, M. Williams, T. M. Filzen, R. I. Fleis, and K. L. Collins. 2005. HIV-1 Nef disrupts antigen presentation early in the secretory pathway. *J Biol Chem* 280: 12840-12848.

34. Williams, M., J. F. Roeth, M. R. Kasper, R. I. Fleis, C. G. Przybycin, and K. L. Collins. 2002. Direct binding of human immunodeficiency virus type 1 Nef to the major histocompatibility complex class I (MHC-I) cytoplasmic tail disrupts MHC-I trafficking. *J Virol* 76: 12173-12184.

35. Specht, A., M. Q. DeGottardi, M. Schindler, B. Hahn, D. T. Evans, and F. Kirchhoff. 2008. Selective downmodulation of HLA-A and -B by Nef alleles from different groups of primate lentiviruses. *Virology* 373: 229-237.

36. Roeth, J. F., M. Williams, M. R. Kasper, T. M. Filzen, and K. L. Collins. 2004. HIV-1 Nef disrupts MHC-I trafficking by recruiting AP-1 to the MHC-I cytoplasmic tail. *J Cell Biol* 167: 903-913.

37. Hubber, A., and C. R. Roy. 2010. Modulation of host cell function by Legionella pneumophila type IV effectors. *Annu Rev Cell Dev Biol* 26: 261-283.

38. Liu, J., D. Shaji, S. Cho, W. Du, J. Gervay-Hague, and R. R. Brutkiewicz. 2010. A threonine-based targeting signal in the human CD1d cytoplasmic tail controls its functional expression. *J Immunol* 184: 4973-4981.

39. Moody, D. B., and S. A. Porcelli. 2003. Intracellular pathways of CD1 antigen presentation. *Nat Rev Immunol* 3: 11-22.

40. Boyle, L. H., A. K. Gillingham, S. Munro, and J. Trowsdale. 2006. Selective export of HLA-F by its cytoplasmic tail. *J Immunol* 176: 6464-6472.

41. Lizee, G., G. Basha, J. Tiong, J. P. Julien, M. Tian, K. E. Biron, and W. A. Jefferies. 2003. Control of dendritic cell cross-presentation by the major histocompatibility complex class I cytoplasmic domain. *Nat Immunol* 4: 1065-1073.

42. Park, B., S. Lee, E. Kim, S. Chang, M. Jin, and K. Ahn. 2001. The truncated cytoplasmic tail of HLA-G serves a quality-control function in post-ER compartments. *Immunity* 15: 213-224.

FOOTNOTES

[1]This work was supported by National Institutes of Health (NIH) Grant R01 AI031168 (to P.P.), Grant R01 GM038093 (to F.B.) NIH Ruth L. Kirschstein National Research Service Award Individual Postdoctoral Fellowship F32 AI089085 (to A.G.) and NIH training grant T32 AI07290 (to A.G.). This project was also funded in part by Yerkes Base Grant ORIP/OD P51OD011132.

[2]Current address:
University of Michigan Medical School, University of Michigan, 1500 East Medical Center Drive, Ann Arbor, MI 48109

[3]Current address:
Division of Biosciences, University College London, Gower Street, London, WC1E 6BT, UK

[4]Address correspondence and reprint requests to Dr. Peter Parham, Department of Structural Biology, Stanford University, Fairchild D-159, 299 Campus Drive West, Stanford, CA 94305. E-mail address: peropa@stanford.edu

[5]Abbreviations used in this paper: ER, endoplasmic reticulum; IP, immunoprecipitation; ALpoly, rabbit anti-Patr-AL polyclonal antibody; ROI, region of interest; BLCL, B lymphoblastoid cell line; TM, transmembrane region.

FIGURE LEGENDS

Figure 1: Cell-surface expression of Patr-AL is very low compared to HLA-A and Patr-A.

Panels A-C) Surface staining, with anti-Patr-AL monoclonal antibody 10A5 (A), anti-MHC class I monoclonal antibody W6/32 (B) or anti-HLA-E monoclonal antibody 3D12 (C), of 221 cells (221, shaded gray), and 221 cells transfected with Patr-AL expressing its native Leader peptide (AL, orange), Patr-AL expressing a mutated Leader that abrogates expression of HLA-E (AL [P2T], blue), HLA-A*02:07 (HLA-A, green) and Patr-A*04:02 (Patr-A, purple). The bar graph on the left shows the median fluorescence intensity (mfi) values obtained for the histograms shown on the right. Error bars indicate standard deviation between two replicates within an experiment. Histograms show staining intensity for intact, live cells. One representative experiment is shown from the three total performed. Not shown are data for 221 transfectants expressing other human (HLA-A*01:01, -A*02:01, -A*02:07, and -A*03:01) and chimpanzee (Patr-A*04:02, -A*05:01, -A*06:01, -A*10:01, -A*11:01, -A*13:01, -A*16:01, and -A*20:01) MHC-A allotypes which have expression levels comparable to the HLA-A*02:07 and Patr-A*24:02 transfectants.

Panel D) Summary of the binding reactions of 10A5 and W6/32 antibodies to microbeads, individually coated with one of 31 HLA-A, 50 HLA-B and 16 HLA-C allotypes. Antibody 10A5 bound to none of the HLA class I allotypes, whereas W6/32 bound to all of them and to similar extent (<15% variation between the beads). Data from at least 100 beads were obtained for each HLA class I allotype.

Figure 2: Patr-AL is not expressed constitutively on cell surfaces.

Upper panels) Cell-surface staining and flow cytometric analysis of ten B lymphoblastoid cell lines (BLCL) derived from chimpanzee peripheral blood B cells. The cells were stained with Patr-AL specific antibody 10A5 (panel A) and pan MHC class I specific antibody W6/32 (panel B). For 10A5 staining (panel A) the bars show the frequency of antibody-binding intact, live cells. For W6/32 staining (panel B) the bars show mean fluorescent intensity (mfi) staining of the intact, live cells. Light gray shaded bars denote BLCL derived from chimpanzees that lack the *Patr-AL* gene, dark gray shaded bars denote BLCL derived from chimpanzees that carry the *Patr-AL* gene.

Lower panels) Shown are analyses comparable to those depicted in the upper panels but performed on samples of peripheral blood mononuclear cells (PBMC) obtained from 24 chimpanzees. Panel C shows the frequency of cells staining for Patr-AL with the 10A5 antibody. Panel D shows the mean frequency intensity (mfi) of staining for MHC class I as detected with the W6/32 antibody.

Panels E-F) Multi-color immunofluorescence staining and confocal microscopy of chimpanzee BLCL derived from a Patr-AL^{+} individual, Miss Eve (left panel) and a Patr-AL^{-} individual, Faye (right panel) fixed with 70% methanol 30% acetone and stained with various antibodies. Patr-AL was stained with ALpoly, (polyclonal Patr-AL-specific rabbit antibodies, in green). The specificity of ALpoly was confirmed by the negative staining of 221 cells (data not shown) and BLCL derived from a Patr-AL^{-} donor. Invariant chain was stained with the PIN.1 monoclonal antibody, which identifies the ER and early ER-derived vesicles of the endolysosomal system (in red). TOTO-3 (in blue) is used as a nuclear counterstain.

Figure 3: Transfected cells make comparable amounts of Patr-AL and HLA-A*02 but Patr-AL mainly stays inside the cell whereas HLA-A*02 goes to the surface

Flow cytometric analysis of 221 cells (221), 221 transfectants expressing Patr-AL (AL) and 221 transfectants expressing HLA-A*02:07 (A*02) after staining with anti-Patr-AL (10A5) and anti-HLA-A*02 (BB7.2) monoclonal antibodies. The upper panels show cell-surface staining for Patr-AL (panel A) and HLA-A*02 (panel B). The bars give the median fluorescence intensity (mfi) values of positively-staining intact, live cells. Error bars represent standard deviation between mfi shown for the data from three replicate experiments.

The lower panels compare the amounts of Patr-AL (panel C) and HLA-A*02 (panel D) that are at intracellular and cell-surface locations. Because of the different physico-chemical properties of the 10A5 and BB7.2 antibodies, different protocols were used in order to detect their epitopes. For 10A5 staining (panel C) cells were fixed with 70% methanol 30% acetone, after which one aliquot of cells was permeabilized with cold acetone and the other was not. The cells were then stained with 10A5 and analyzed by flow cytometry. For BB7.2 staining (panel D), transfectants were fixed with 4% paraformaldehyde, after which one aliquot of cells was permeabilized with 0.04% saponin in FACS Buffer and the other was not. The cells were then stained with the BB7.2 antibody and analyzed by flow cytometry. In panels C and D, gray bars give the staining of non-permeabilized cells and black bars show the staining of the permeabilized cells. Error bars show the standard deviation in mfi for data from three replicate experiments.

Figure 4: Patr-AL concentrates in the endoplasmic reticulum and the cis-Golgi.

Panels A-D) Multi-color immunofluorescence staining and confocal microscopy of 221-Patr-AL transfectants (left panels) fixed with 70% methanol 30% acetone and stained with various antibodies. Patr-AL was stained with ALpoly, (polyclonal Patr-AL-specific rabbit antibodies). The specificity of ALpoly was confirmed by the negative staining of 221 cells (data not shown). HLA-DR is stained with the L243 monoclonal antibody, which recognizes mature class II molecules that lack the invariant chain. Invariant chain is stained with the PIN.1 monoclonal antibody. Golgi matrix protein of 130 kD is stained with the GM130 monoclonal antibody. In the panels at the right are scattergrams showing the quantitative co-localization analysis of pairs of markers. Numbers in the scattergram are Pearson's correlation coefficient values for the indicated channels (1 = perfect colocalization, 0 = no colocalization, -1 = negative colocalization) as averaged from analysis of 50 cells. Scale bar = 5μm. For all figures, blue = DNA.

Panel E) Patr-AL was immunoprecipitated from Patr-AL transfected 221 cells (221-AL) using the 10A5 antibody and the Dynabeads® Co-Immunoprecipitation Kit (Invitrogen). 221 cells served as the negative control. Immunoprecipitates were treated with Endoglycosidase H (1000U) (+), or not (-), and analyzed by SDS-PAGE on a 4-15% gradient gel. Western blotting was performed using ALpoly to detect Patr-AL (shown on the left). For comparison, total lysates of 221 and 221-AL cells were similarly analyzed by SDS-PAGE and Western blotting (shown on the right).

Panel F) Multi-color immunofluorescence staining and confocal microscopy of 221 cells transfected with Patr-AL. Cells were fixed (as described above) simultaneously stained with

ALpoly (green), anti-lysosomal and anti-late endosomal marker, Lamp-1 (red) and HLA-DR (blue). The Lamp-1^+ and HLA-DR^+ compartments within each cell were analyzed by quantitative colocalization analysis of pairwise comparisons for each of the three channels imaged. Pink color shows overlap of red and blue staining.

Panel G) From the data illustrated in panel F, mean values for Pearson's correlation coefficient were calculated from pairwise comparisons of fluorescence intensity measurements, of 20 cells, from each of the 3 channels imaged. Error bars represent standard deviation between average Pearson's correlation coefficient values for the 20 cells sampled.

Figure 5: Cell surface expression of Patr-AL, but not HLA-A*02, is temperature sensitive

221 cells transfected with Patr-AL (upper panel) and HLA-A*02 (lower panel) were cultured in complete RPMI medium and incubated for 16 hours at various temperatures from 21-37°C. Cell surface expression of Patr-AL (10A5) and HLA-A*02:07 (BB7.2) were subsequently assayed by antibody staining and flow cytometry. The average mfi values for positively-staining, live cells are plotted. Error bars represent standard deviation between mfi shown for the data from 3 replicate experiments.

Figure 6: Unique features in the cytoplasmic tail contribute to the intracellular retention of Patr-AL.

Panel A) Amino-acid sequence alignment of the cytoplasmic tails from Patr-AL and other human and chimpanzee MHC class I molecules. Shaded gray are positions 321, 326, 329 and 333 where Patr-AL has a unique combination of amino-acid residues.

Panel B) 221 cells transfected with either Patr-AL (AL) or a mutant of Patr-AL (AL^{cytA2}) having the cytoplasmic tail of HLA-A*02 were stained with anti-Patr-AL antibody (10A5) and analyzed by flow cytometry. Panel C) 221 cells transfected with HLA-A*02 (A*02) or a mutant of HLA-A*02 ($A*02^{cytAL}$) having the cytoplasmic tail of Patr-AL were stained with anti-HLA-A*02 antibody (BB7.2) and analyzed by flow cytometry. For 10A5 binding (panel B) and BB7.2 binding (panel C) the average mfi value of cells is plotted. Error bars represent the standard deviation between mfi for the data from three replicate experiments. *** = $p \leq 0.0005$.

Figure 7: The four residues that distinguish the cytoplasmic tail of Patr-AL all contribute to the intracellular retention of Patr-AL.

Patr-AL, HLA-A*02:07 and mutants of them that represent all 16 combinations of the natural polymorphisms at positions 321, 326, 329 and 333 were transiently transfected into HeLa cells. Each wild-type and mutant contained 3xFLAG epitopes at the amino-terminus which enabled their surface expression to be compared using the anti-3xFLAG antibody and flow cytometric analysis. Within each panel a subgroup of the mutants are compared to the Patr-AL full tail mutant (left panels) and wild-type HLA-A*02:07 (right panels). Shown on the far left are the sequence motifs at positions 321, 326, 329 and 333 shared by the Patr-AL and HLA-A*02 paired in each row. Orange boxes denote residues naturally occurring in Patr-AL; blue boxes denote residues naturally occurring in HLA-A*02. Panel A mutants have one residue shared with Patr-AL and three with HLA-A*02. Panel B mutants have two residues shared with Patr-AL and two with HLA-A*02. Panel C mutants have three residues shared with Patr-AL and one with HLA-A*02. In each panel the horizontal bars give the levels of cell-surface expression as mfi. At least

3 replicates were analyzed for each mutant. Values that are statistically different from the HLA-A*02 cytoplasmic tail are: **** = $p < 0.0001$, *** = $p < 0.0005$, ** = $p < 0.005$, * = $p < 0.05$. These values were calculated by one-way ANOVA for each pairwise comparison.

Figure 8: Natural variation at position 295 of the transmembrane region affects expression of HLA-A*02 but not Patr-AL.

Patr-AL and HLA-A*02:07 differ at position 295 in the transmembrane region as well as at four positions in the cytoplasmic domain. For both Patr-AL and HLA-A*02, mutants were made to give all combinations of the transmembrane region and cytoplasmic domain. Mutant construction, analysis of cell-surface expression and calculation of significance values were as described in the legend to Figure 7. At least 3 replicates were analyzed for each mutant.

Figure 9: The cytoplasmic tails of MHC class I molecules contain sorting motifs contributing to their patterns of intracellular trafficking.

The cytoplasmic tail sequence and motif contents are compared among Patr-AL and human MHC class I molecules. Cytoplasmic tails of MHC class I molecules differ in length and in their contents of intracellular sorting motifs. All sorting motifs are shaded gray, with the exception of the Patr-AL-specific motif, which is shaded light orange. Functionally important residues within each motif are colored red. One motif is highlighted per tail sequence. Numbers on the scale represent the position within the cytoplasmic tail of Patr-AL. References for each motif described are also noted. (27, 28, 38-42)

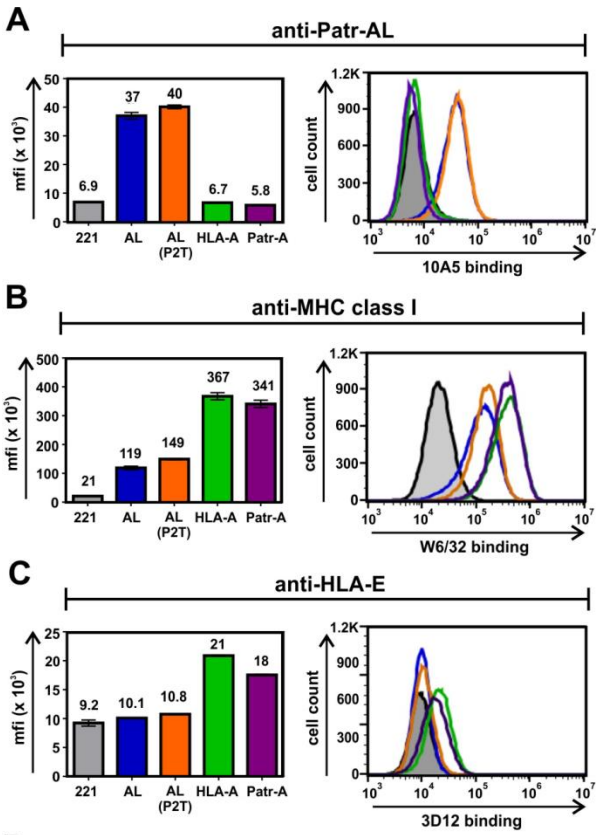

D

Comparison of 10A5 and W6/32 binding to HLA-A, -B and -C

HLA (# allotypes)	Antibody	Range		Mean
		Min	Max	
HLA-A (31)	10A5	10	46	23
	W6/32	22,960	23,612	23,225
HLA-B (50)	10A5	9	71	30
	W6/32	22,002	28,136	23,226
HLA-C (16)	10A5	34	77	49
	W6/32	17,715	23691	21,989

Figure 1

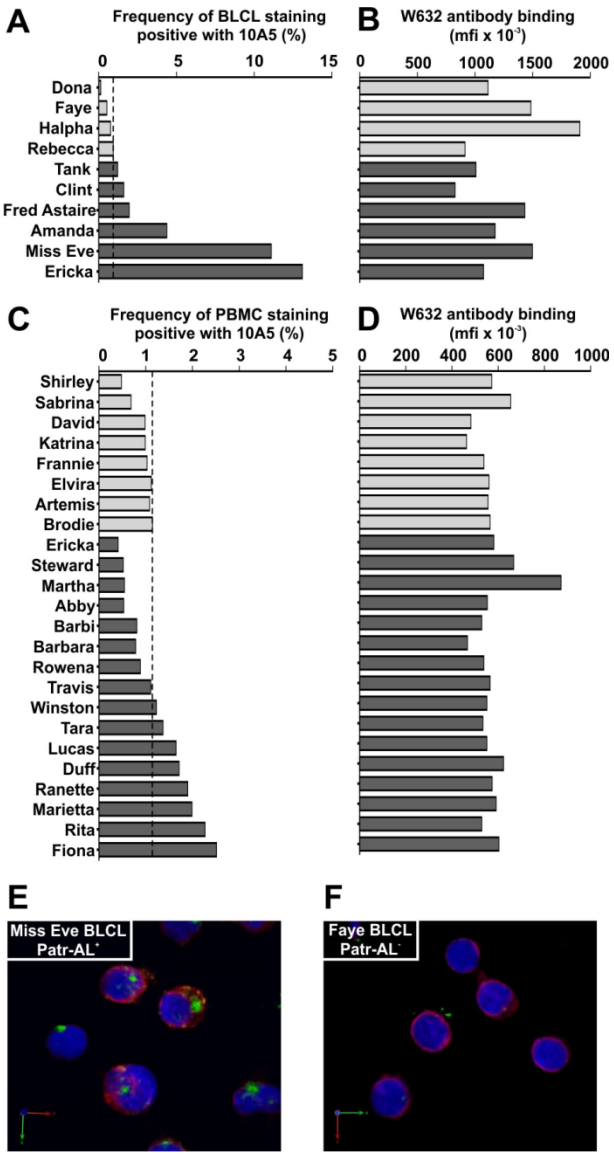
A
Frequency of BLCL staining positive with 10A5 (%)
0
5
10
15
Dona
Faye
Halpha
Rebecca
Tank
Clint
Fred Astaire
Amanda
Miss Eve
Ericka
B
W632 antibody binding (mfi x 10-3)
0
500
1000
1500
2000
C
Frequency of PBMC staining positive with 10A5 (%)
0
1
2
3
4
5
Shirley
Sabrina
David
Katrina
Frannie
Elvira
Artemis
Brodie
Ericka
Steward
Martha
Abby
Barbi
Barbara
Rowena
Travis
Winston
Tara
Lucas
Duff
Ranette
Marietta
Rita
Fiona
D
W632 antibody binding (mfi x 10-3)
0
200
400
600
800
1000
E
Miss Eve BLCL Patr-AL+
F
Faye BLCL Patr-AL-

Figure 2

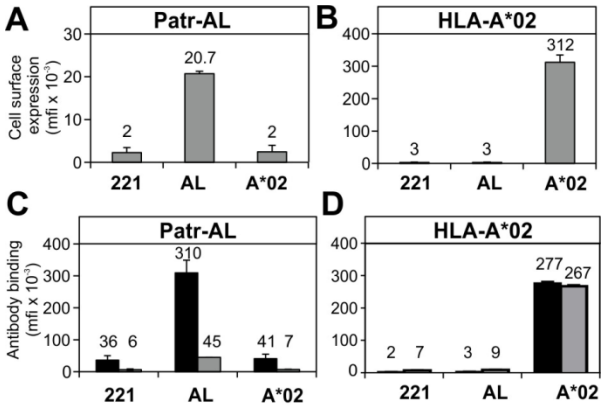
A
Patr-AL
Cell surface expression (mfi x 10^{-3})
30
20
10
0
2
20.7
2
221
AL
A*02
B
HLA-A*02
400
300
200
100
0
3
3
312
221
AL
A*02
C
Patr-AL
Antibody binding (mfi x 10^{-3})
400
300
200
100
0
36 6
310
45
41 7
221
AL
A*02
D
HLA-A*02
400
300
200
100
0
2 7
3 9
277
267
221
AL
A*02

Figure 3

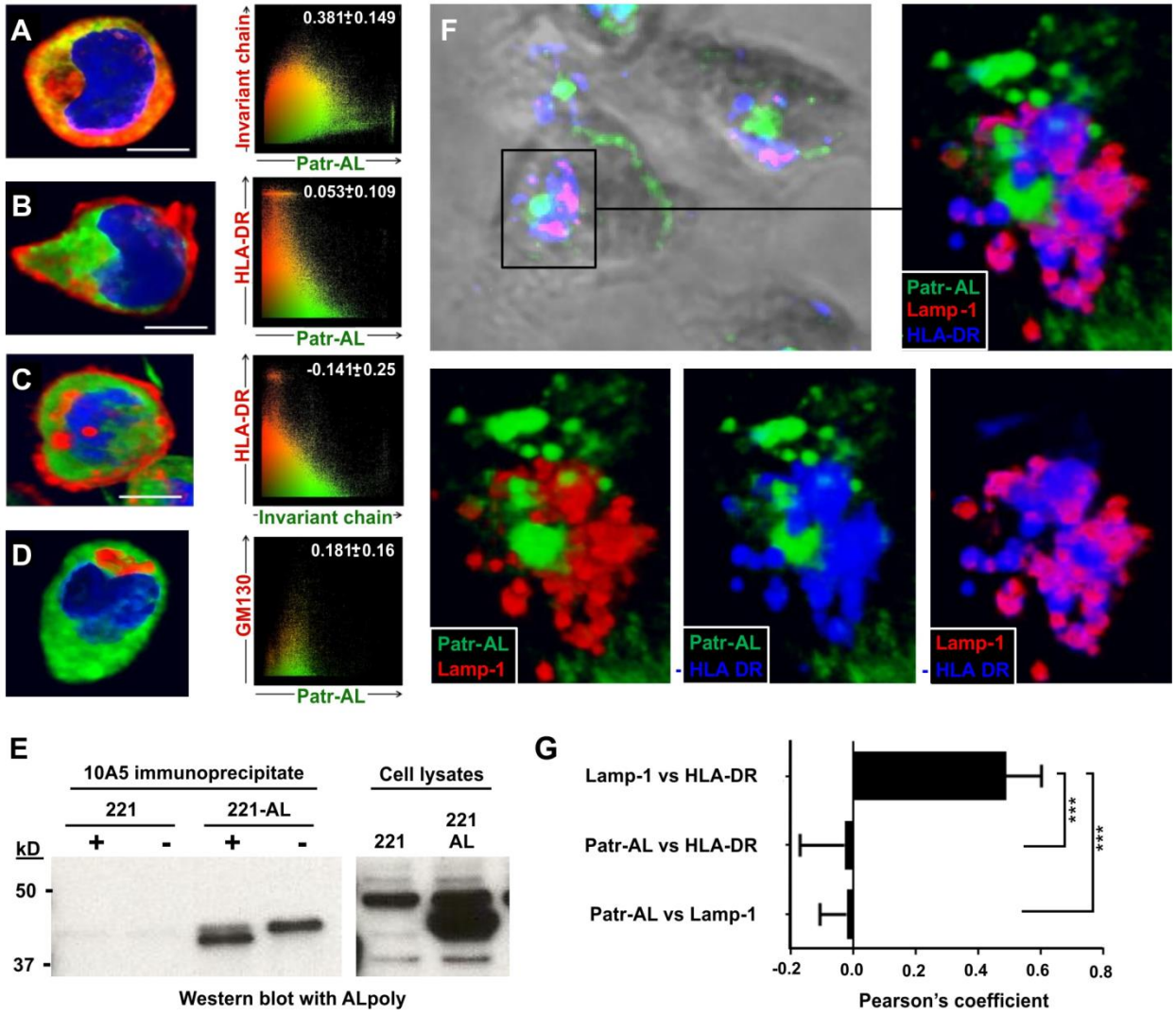
A
B
C
D
Invariant chain
Patr-AL
0.381±0.149
HLA-DR
Patr-AL
0.053±0.109
HLA-DR
Invariant chain
-0.141±0.25
GM130
Patr-AL
0.181±0.16
F
Patr-AL
Lamp-1
HLA-DR
Patr-AL
Lamp-1
Patr-AL
HLA DR
Lamp-1
HLA DR
E
10A5 immunoprecipitate
Cell lysates
221
221-AL
221
221 AL
kD
+
-
+
-
50
37
Western blot with ALpoly
G
Lamp-1 vs HLA-DR
Patr-AL vs HLA-DR
Patr-AL vs Lamp-1
***
***
-0.2
0.0
0.2
0.4
0.6
0.8
Pearson's coefficient

Figure 4

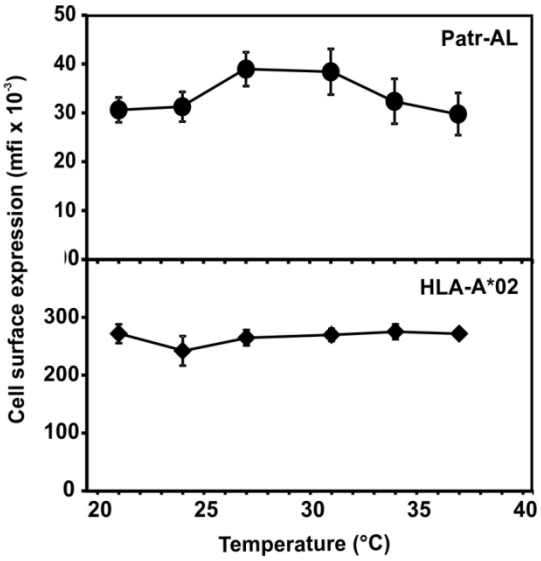
Patr-AL
HLA-A*02
Cell surface expression (mfi x 10-3)
Temperature (°C)
50
40
30
20
10
0
300
200
100
0
20
25
30
35
40

Figure 5

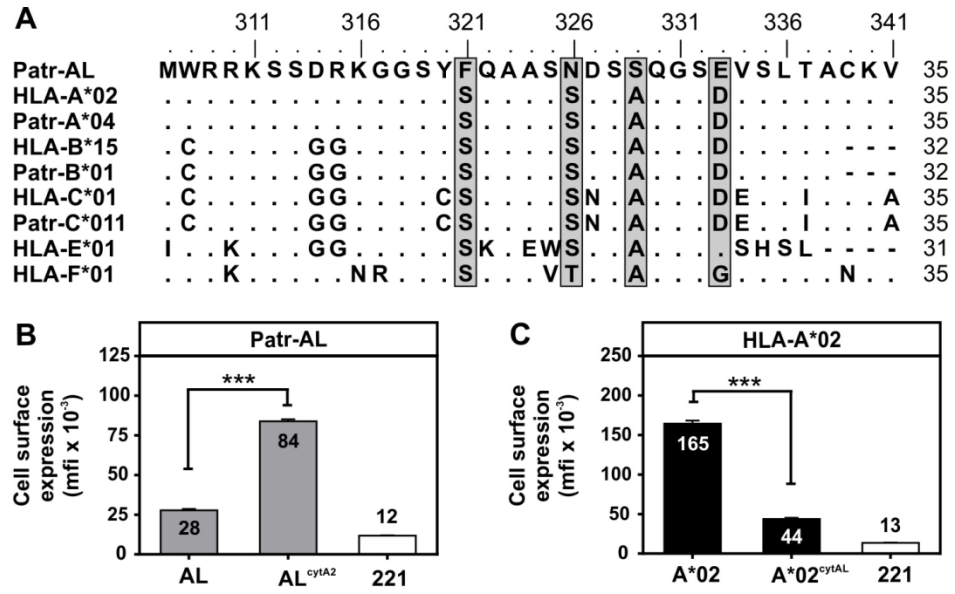
A
311
316
321
326
331
336
341
Patr-AL MWRRKSSDRKGGSYFQAASNDSSQGSEVSLTACKV 35
HLA-A*02 S S A D 35
Patr-A*04 S S A D 35
HLA-B*15 C GG S S A D - - - 32
Patr-B*01 C GG S S A D - - - 32
HLA-C*01 C GG CS SN A DE I A 35
Patr-C*011 C GG CS SN A DE I A 35
HLA-E*01 I K GG SK EW S A SHSL - - - - 31
HLA-F*01 K NR S VT A G N 35
B
Patr-AL
Cell surface expression (mfi x 10-3)
125
100
75
50
25
0
***
84
28
12
AL
ALcytA2
221
C
HLA-A*02
Cell surface expression (mfi x 10-3)
250
200
150
100
50
0
***
165
44
13
A*02
A*02cytAL
221

Figure 6

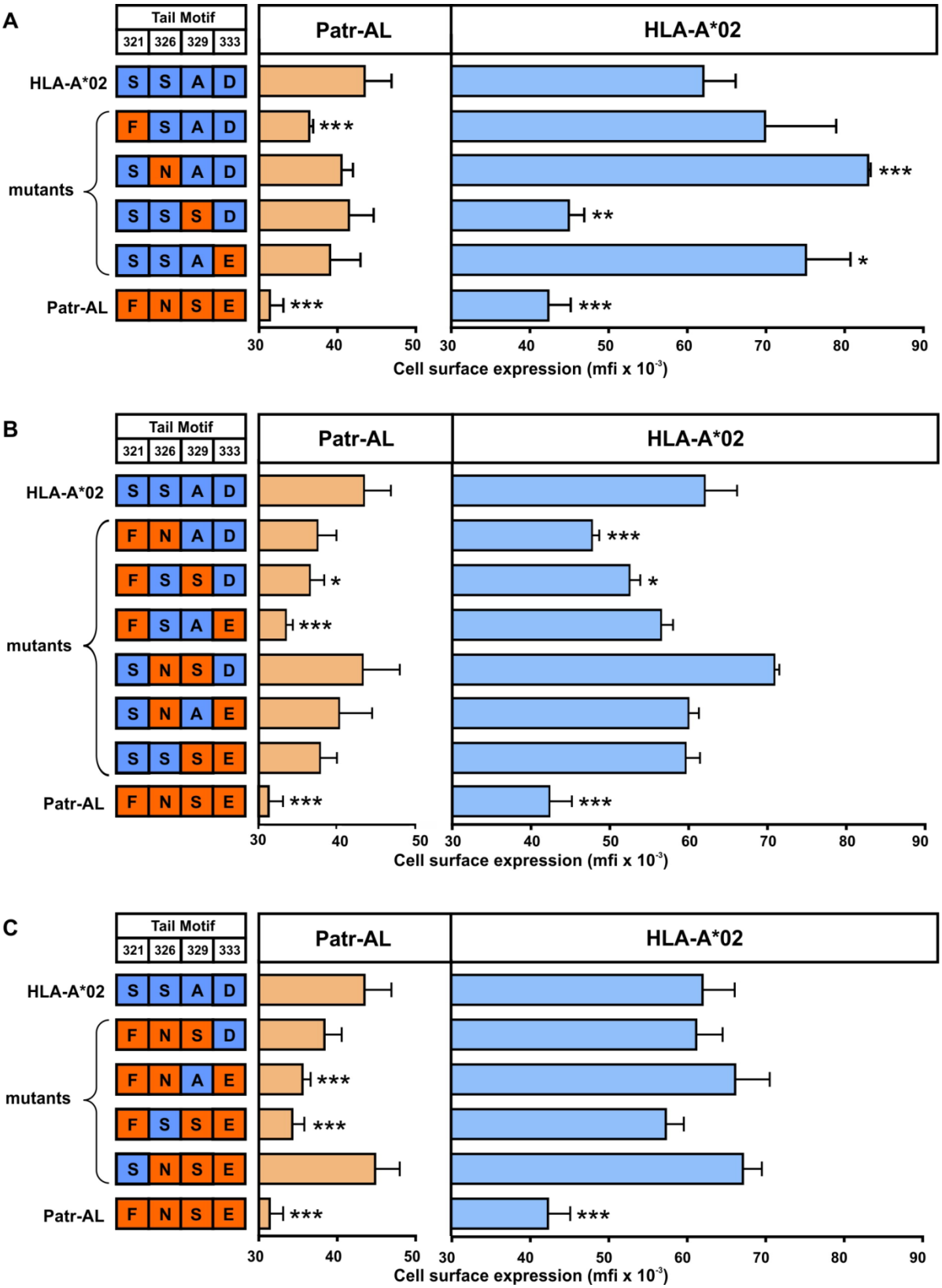
A
Tail Motif
321 326 329 333
Patr-AL
HLA-A*02
HLA-A*02
S S A D
mutants
F S A D
S N A D
S S S D
S S A E
Patr-AL
F N S E
***
***
**
*
***
30 40 50
30 40 50 60 70 80 90
Cell surface expression (mfi x 10-3)
B
Tail Motif
321 326 329 333
Patr-AL
HLA-A*02
HLA-A*02
S S A D
mutants
F N A D
F S S D
F S A E
S N S D
S N A E
S S S E
Patr-AL
F N S E
***
*
***
***
*
***
30 40 50
30 40 50 60 70 80 90
Cell surface expression (mfi x 10-3)
C
Tail Motif
321 326 329 333
Patr-AL
HLA-A*02
HLA-A*02
S S A D
mutants
F N S D
F N A E
F S S E
S N S E
Patr-AL
F N S E
***
***
***
***
30 40 50
30 40 50 60 70 80 90
Cell surface expression (mfi x 10-3)

Figure 7

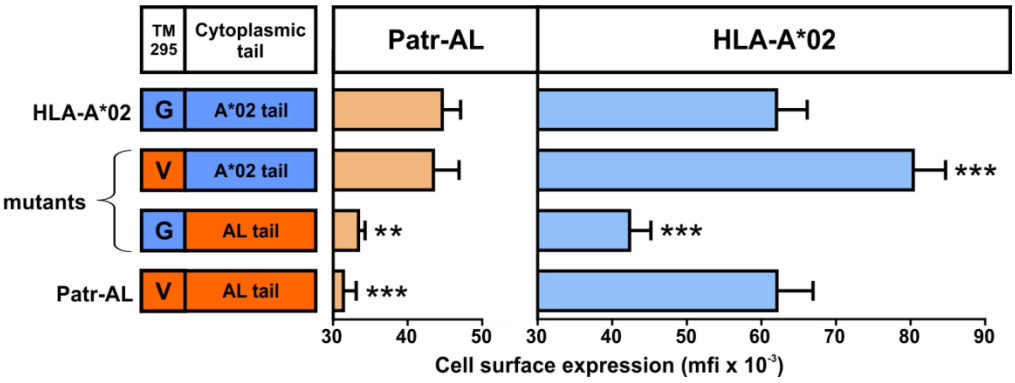
TM 295
Cytoplasmic tail
Patr-AL
HLA-A*02
HLA-A*02
G
A*02 tail
mutants
V
A*02 tail
G
AL tail
Patr-AL
V
AL tail
**
***
***
***
30
40
50
30
40
50
60
70
80
90
Cell surface expression (mfi x 10-3)

Figure 8

MHC class I molecule	Length of cytoplasmic tail	Location of motif in cytoplasmic tail	Type of motif
MICA*001	45	E E L V Q V L D Q H P V G D D L G F Q P D	Dihydrophobic basolateral sorting motif [28]
CD1d	14	T F K R S Y Q G V L T F K R S Y Q G V L	Threonine-based cell surface targeting motif [38] Tyrosine-based endosomal targeting motif [39]
CD1c	14	V F K K S Y Q D I L	Tyrosine-based endosomal targeting motif [39]
CD1b	14	A Y M R S Y Q N I P	Tyrosine-based endosomal targeting motif [39]
CD1a	10	A F R K F C	-
HLA-G	8	L K K S	Dilysine ER retrieval motif [42]
HLA-F	35	M K K S R N R G S Y S Q A T A G V S L T V M K K S R N R G S Y S Q A T A G V S L T V M K K S R N R G S Y S Q A T A G V S L T V	RxR motif forward transport motif [40] Tyrosine-based endosomal targeting motif [41] C-terminal valine ER export motif [40]
HLA-E	31	I K K S G K G G S Y S K A S A E S H S L	Tyrosine-based endosomal targeting motif [41]
HLA-C*01	35	M R K S G K G G S C S Q A S A D E S L I A M R K S G K G G S C S Q A S A D E S L I A	Dihydrophobic internalization motif [27] Lysosomal targeting motif [27]
HLA-A*02	35	M R K S R K G G S Y S Q A S A D V S L T V	Tyrosine-based endosomal targeting motif [41]
Patr-AL	35 35	M R K S R K G G S Y F Q A N S E V S L T V M R K S R K G G S Y F Q A N S E V S L T V	Tyrosine-based endosomal targeting motif [41] Patr-AL-specific motif

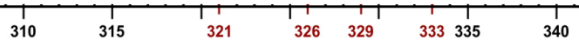

Position numbers refer to the Patr-AL sequence

Figure 9

3xFLAG-tag Cloning Primers

Primer name	Primer sequence
HindIII-AL-L-KZ-F	5 '- AGCAAAGCTTCACCATGGCCGTCATGGCTCCTCG - 3'
HindIII-A0207-L-KZ-F	5' - AGCAAAGCTTCACCATGGCCGTCATGGCGCCCCG - 3'
3xFLAG-AL-F	5’ - ATTATAAAGATCATGACATCGATTACAAGGATGACGATGACAAGGGCTCCCACTCCATGAGGTA - 3’
3xFLAG-A-F	5’ - ATTATAAAGATCATGACATCGATTACAAGGATGACGATGACAAGGGCTCTCACTCCATGAGGTA - 3’
3xFLAG-ALL-R	5’ - TCGATGTCATGATCTTTATAATCACCGTCATGGTCTTTGTAGTCCGCCCAGGTCTGGGTCAGGG - 3’
XbaI_AL-A_Cyt_R	5' - GGCGTCTAGAGCTCACACTTTACAAGCTGTG - 3'

Figure S1: 3xFLAG-tag cloning primers.

Listed are primers used to generate FLAG-tagged Patr-AL and HLA-A*02 by a three-step PCR approach.

Mutagenesis primers

Primer name	Primer sequence
AL2_AS	5' - CTTGCAGCCTGAGAGTAGCTCCCTCCTTTTCTATCT - 3'
AL3_AS	5' - CCCTGGGAACTGTCACTGCTTGCAGCCTGAAAG - 3'
AL4_AS	5' - GAGCCCTGGGCACTGTCATTGCTTGCAGCC - 3'
AL5_AS	5' - GCTGTGAGAGACACATCAGAGCCCTGGGA - 3'
AL6_AS	5' - CCTGGGAACTGTCACTGCTTGCAGCCTGAGA - 3'
AL7_AS	5' - GAGCCCTGGGCACTGTCATTGCTTGCAGCC - 3'
AL8_AS	5' - CTTGCAGCCTGAGAGTAGCTCCCTCCTTTTCTATCT - 3'
AL9_AS	5' - AGCCCTGGGCACTGTCACTGCTTGCAGCCTGAGAG - 3'
AL10_AS	5' - GCTGTGAGAGACACATCAGAGCCCTGGGA - 3'
AL11_AS	5' - GAGCCCTGGGCACTGTCATTGCTTGCAGCC - 3'
AL12_AS	5' - CCTGGGCACTGTCACTGCTTGCAGCCTGAAA - 3'
AL13_AS	5' - CCCTGGGAACTGTCACTGCTTGCAGCCTGAAAG - 3'
AL14_AS	5' - GAGCCCTGGGCACTGTCACTGCTTGCAGCCTGAAAGTA - 3'
AL15_AS	5' - GAGCCCTGGGCACTGTCATTGCTTGCAGCC - 3'
AL-A-TM	5' - GTGATCACAGCTCCAAAGAGAACCAGGCCAGCAATGATG - 3'
A2_AS	5' - CTTGCAGCCTGAAAGTAGCTCCCTCCTTTTCTATCT - 3'
A3_AS	5' - CTGGGCACTGTCATTGCTTGCAGCCTGAG - 3'
A4_AS	5' - GAGCCCTGGGAACTGTCACTGCTTGCAGCC - 3'
A5_AS	5' - GCTGTGAGAGACACCTCAGAGCCCTGGGC - 3'
A6_AS	5' - GAGCCCTGGGAACTGTCACTGCTTGCAGCC - 3'
A7_AS	5' - CTGGGCACTGTCATTGCTTGCAGCCTGAG - 3'
A8_AS	5' - CCTGGGAACTGTCATTGCTTGCAGCCTGAGA - 3'
A9_AS	5' - GAGCCCTGGGAACTGTCATTGCTTGCAGCC - 3'
A10_AS	5' - GCTGTGAGAGACACCTCAGAGCCCTGGGC - 3'
A11_AS	5' - GAGCCCTGGGAACTGTCACTGCTTGCAGCC - 3'
A12_AS	5' - CTTGCAGCCTGAAAGTAGCTCCCTCCTTTTCTATCT - 3'
A13_AS	5' - GAGCCCTGGGAACTGTCACTGCTTGCAGCC - 3'
A14_AS	5' - AGCCCTGGGAACTGTCATTGCTTGCAGCCTGAGAG - 3'
A15_AS	5' - CCTGGGCACTGTCATTGCTTGCAGCCTGAAA - 3'
A-AL-TM	5' - GTGATCACAGCTACAAACAGAACCAGGCCAGCAATGATG - 3'

Figure S2: Site-directed mutagenesis primers.

Listed are primers used to mutate specific residues in the transmembrane and cytoplasmic tails of 3xFLAG-tagged-Patr-AL or -HLA-A*02 by site-directed mutagenesis.

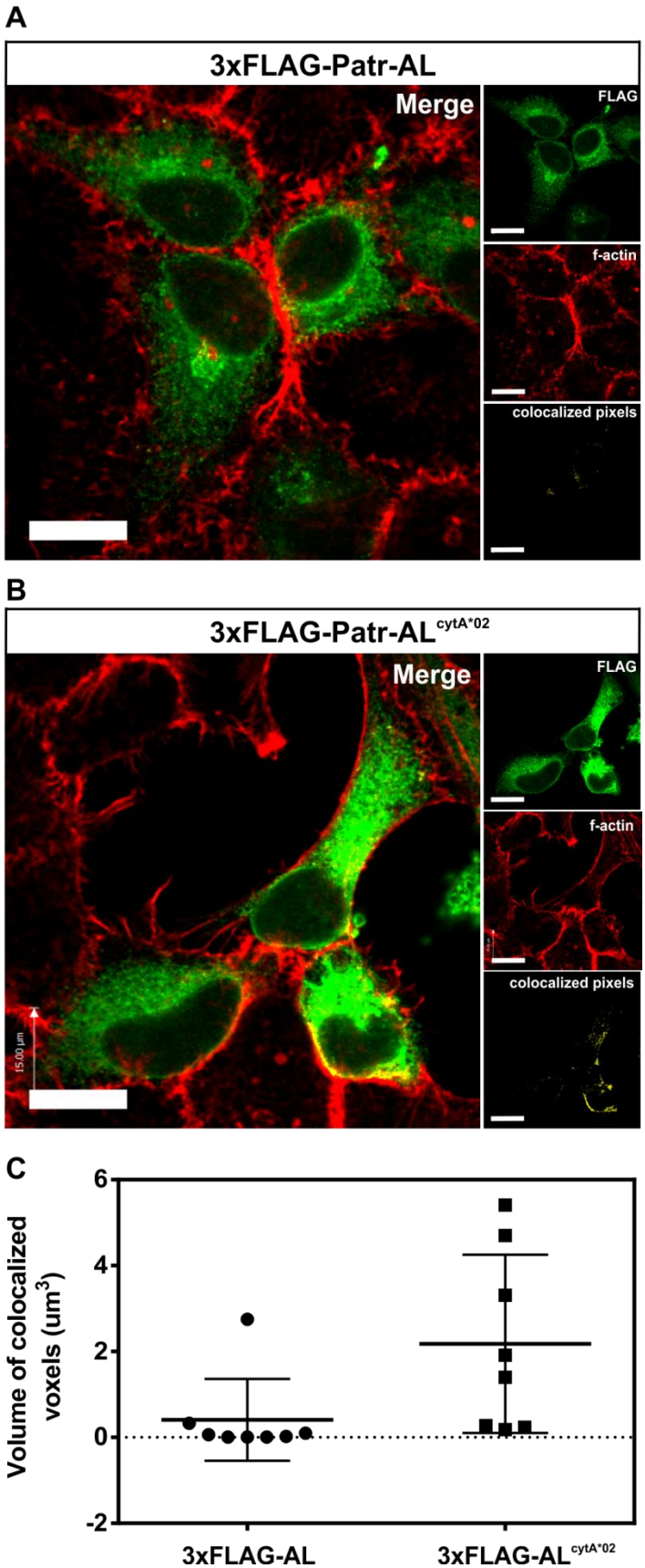

Figure S3: A small amount of Patr-AL is detected on the cell surface by high resolution confocal microscopy.

Panels A and B) HeLa were transiently transfected with plasmids expressing either 3xFLAG-tagged Patr-AL or its cytoplasmic tail swap mutant, 3xFLAG-tagged Patr-AL^{cytA*02}. 2 days post-transfection cells were fixed with 4% paraformaldehyde and stained with an anti-3xFLAG rabbit polyclonal antibody (Sigma-Aldrich) and the bicyclic peptide, phalloidin, to stain f-actin as a marker of the cell surface. Quantitative colocalization analysis in 3 dimensions was performed between the two channels and colocalized voxels identified. The large image in panels A and B represents a merge between the colocalized voxels and the 2 channels imaged, whereas images from individual channels and colocalized pixels are shown on the right. Scale bar = 15µm.

Panel C) The total volume of colocalized voxels per cell is calculated for 8 cells from each transfection. A small, but measurable, amount of cell surface Patr-AL is detected on the cell surface by microscopy, when compared to Patr-AL's cytoplasmic tail mutant, consistent with flow cytometry analysis of stable 221 transfectants (Fig. 6B and C).

A

Organism	Protein	Cytoplasmic tail motiff 321	326	329	333	# allotypes (total)
Hominoids						
chimpanzee	Patr-AL	**F**	**N**	**S**	**E**	all
human	HLA-A	S	S	A	D	129 (173)
		T	S	A	D	44 (173)
	HLA-B	S	S	A	D	all (293)
	HLA-E	S	S	A	▪	9 (9)
gorilla	Gogo-B*07:01	S	S	A	▪	1 (9)
orangutan	Popy-A	S	▪	A	D	7 (7)
	Popy-E	S	S	A	▪	1 (1)
	Poab-A	S	▪	A	D	1 (1)
Old world monkeys						
Rhesus macaque	Mamu-B	S	S	A	D	126
		S	▪	A	D	64
		▪	▪	A	D	9
		▪	S	A	▪	4
		▪	S	A	D	3
	Mamu-A	S	S	A	D	224
	Mamu-A1*043:05	▪	S	A	D	1
	Mamu-E*02:04, *02:05	S	S	▪	D	2
Crab-eating macaque	Mafa-B	S	S	A	D	84
		S	▪	A	D	46
		▪	▪	A	D	9
		▪	S	A	▪	4
		▪	S	A	D	2
	Mafa-A	S	S	A	D	153
	Mafa-A1*070,*071	S	▪	A	D	2
Southern pig-tailed macaque	Mane-B	S	S	A	D	49
		S	▪	A	D	19
		▪	▪	A	D	5
		▪	S	A	▪	1
	Mane-A	S	S	A	D	25
	Mane-A2*05:18	▪	S	A	D	1
	Mane-E*02:06	S	S	▪	D	1
Stump-tailed macaque	Maar-B	S	S	A	D	4
		▪	▪	A	D	1
Assam macaque	Maas-B	S	S	A	D	7
		▪	▪	A	D	2
		S	▪	A	D	1
Tibetan macaque	Math-B	S	S	A	D	11
	Math-B,-I	S	▪	A	D	5 (B), 1 (I)
	Math-B	▪	▪	A	D	1
grivet	Chae-MHC-FB12-6	▪	▪	A	D	1
Olive baboon	Paan-Bx	S	▪	A	D	1
Yellow baboon	Pacy-B*03	S	▪	A	D	1
New World monkeys						
Squirrel monkey	Sasc-MHCx	▪	S	A	D	1
marmoset	Caja-MHCx	▪	S	A	D	1
	Caja-E	▪	▪	A	D	1
Cotton-top tamarin	Saoe-E*01	▪	▪	A	▪	1
Prosimians						
Pygmy slow loris	Nypy-W01	T	▪	A	D	1 (1)

B

Organism	Protein	Cytoplasmic tail motiff 321	326	329	333	# allotypes (total)
Hominoids						
chimpanzee	Patr-AL	**F**	**N**	**S**	**E**	all
human	HLA-E	S	S	A	▪	9 (9)
orangutan	Popy-E	S	S	A	▪	1 (1)
Old world monkeys						
Rhesus macaque	Mamu-E*02:20	S	S	T	▪	1
	Mamu-E*02:04, *02:05	S	S	▪	D	2
Southern pig-tailed macaque	Mane-E*02:06	S	S	▪	D	1
New World monkeys						
marmoset	Caja-E	▪	▪	A	D	1
Cotton-top tamarin	Saoe-E*01	▪	▪	A	▪	1

Figure S4: The Patr-AL cytoplasmic tail motif is specific to Patr-AL and likely originated in a primordial MHC-E.

The pattern of amino acid substitutions at positions 321, 326, 329 and 333 in jawed vertebrate MHC molecules were analyzed for sequences sharing at least one substitution with Patr-AL residues at these positions. Listed (A) are the protein sequences identified and their respective organisms. The right column shows the number of different sequences within that lineage which contain the depicted tail motif, and in parenthesis is shown the total number of sequences analyzed. If no parenthesis is noted, that was the only sequence identified of that lineage for that organism. Also shown, as the first entry for each lineage, are the number of sequences identified containing the HLA-A characteristic pattern of substitution at these residues. Columns highlighted in light green and containing dots, are residues in common with that of Patr-AL, at that position. Panel (B) demonstrates that all individual substitutions in common with the Patr-AL cytoplasmic tail motif can be found in representative primate MHC-E sequences.